Decreased translation of *Dio3* mRNA is associated with drug-induced hepatotoxicity

Kate M. DUDEK*[1], Laura SUTER†, Veerle M. DARRAS‡, Emma L. MARCZYLO§ and Timothy W. GANT§[1]

*Systems Toxicology Group, Medical Research Council Toxicology Unit, Hodgkin Building, Lancaster Road, Leicester LE1 9HN, U.K., †Institut for Chemistry and Bioanalytics, School of Life Sciences, University of Applied Sciences and Arts Northwestern Switzerland (FHNW), Gründenstrasse 40, 4132 Muttenz, Switzerland, ‡Laboratory of Comparative Endocrinology, Department of Biology, Section Animal Physiology and Neurobiology, KU Leuven, Naamsestraat 61, PB 2464, Leuven, B-3000, Belgium, and §Centre for Radiation, Chemical and Environmental Hazards, Public Health England, Harwell Campus, Didcot, Oxfordshire OX11 0RQ, U.K.

Recent work has demonstrated the importance of post-transcriptional gene regulation in toxic responses. In the present study, we used two rat models to investigate mRNA translation in the liver following xenobiotic-induced toxicity. By combining polysome profiling with genomic methodologies, we were able to assess global changes in hepatic mRNA translation. *Dio3* (iodothyronine deiodinase type III) was identified as a gene that exhibited specific translational repression and had a functional role in a number of relevant canonical pathways. Western blot analysis indicated that this repression led to reduced D3 (the protein expressed by *Dio3*) levels, enhanced over time and with increased dose. Using Northern blotting techniques and qRT-PCR (quantitative reverse transcription–PCR), we confirmed further that there was no reduction in *Dio3* mRNA, suggesting that translational repression of *Dio3* is an important determinant of the reduced D3 protein expression following liver damage. Finally, we show that drug-induced hepatotoxicity appears to cause localized disruptions in thyroid hormone levels in the liver and plasma. We suggest that this leads to reduced translation of *Dio3* mRNA, which results in decreased D3 production. It may therefore be possible that this is an important mechanism by which the liver can, upon early signs of damage, act rapidly to maintain its own energy equilibrium, thereby avoiding global disruption of the hypothalamic–pituitary–thyroid axis.

Key words: InnoMed PredTox consortium, iodothyronine deiodinase type III, liver, polysome profiling, toxicogenomics, translation.

INTRODUCTION

The control of gene expression downstream of transcription is of physiological and toxicological importance due to the speed at which this level of regulation can be used to generate new proteins [1]. Such responses are essential within the CNS (central nervous system), for example, where cells demonstrate rapid variation in their metabolic activity [2,3], and within the liver where a rapid response is necessary to combat the constantly changing chemical milieu. Translational regulation enables a faster, more flexible response to cellular stress because the need to transport newly synthesized mRNAs to make more protein is avoided [3]. This response is demonstrated in cases of temperature shock and DNA damage where the majority of mRNA translation is shut down, with just a few key mRNAs increasing their rates of translation to enable the cell to deal with the additional stress [4]. Analysis of the extent to which mRNAs are recruited to ribosomes gives a quantifiable measure of translation efficiency and is a well-established technique [5]. This process can be coupled with genomics methodologies to allow a global assessment of the translational activity of mRNAs following cellular stress. Furthermore, in combining these data with those obtained from transcriptional studies, a comprehensive overview of the gene-regulatory processes used by the cell to adapt to, and recover from, stress can be obtained. This approach has demonstrated a role for both transcriptional and translational regulation in many pathophysiological states such as drug resistance and cell-cycle control [6,7]. In addition, with miRNAs (microRNAs) and other non-coding RNA species already established as translational regulators [8], research focusing on those regulatory processes occurring at the level of mRNA translation has increased. In fact, in certain cases, this level of control is the primary determinant of gene expression [2,9,10].

To investigate whether such translational mRNA regulation was important following drug-induced hepatotoxicity, we used two *in vivo* models. One of these was developed by the European Union Innovative Medicines Initiative (InnoMed) PredTox consortium. The consortium undertook a series of experiments to investigate liver injury in the rat following dosing with novel pharmaceutical reagents that had failed during development due to overt toxicity [11]. The other was the well-established rat thioacetamide model [12,13], which we have included to supplement and verify the findings from the PredTox model. Using polysome fractionation and microarray methods, we were able to globally analyse differential mRNA translation, and through subsequent pathway analysis with Ingenuity IPA software (Ingenuity® Systems), we explored canonical pathways of potential interest and relevance in cases of hepatotoxicity. We identified *Dio3* (iodothyronine deiodinase type III) as one of the genes that exhibited specific translational control under conditions of hepatic toxicity.

Dio3 encodes an enzyme (D3) that is vital for TH (thyroid hormone) regulation; the maintenance of TH levels throughout life is of fundamental importance. The two major THs are T_4

(thyroxine), secreted by the thyroid gland, and its biologically active form, T_3 (3,5,3′-triiodothyronine). In combination, these two molecules play a critical role during development, cellular proliferation and metabolic homoeostasis [14–16], and even transient disruptions in their levels can cause a wide number of transcriptional gene changes [17]. Prolonged deficiency causes growth retardation, impaired cognitive function and, in severe cases, infantile haemangioma [18,19]. In addition to D3, there are two further deiodinases (D1 and D2), all of which are highly conserved throughout the vertebrate kingdom [20]. Of the two THs, T_4 is the most abundant; it is transported through the cellular membrane, via membrane transporters, before diffusion to the nucleus where it is converted into the more active T_3 by D1 and D2 [21]. On a tissue-specific basis, if levels of T_3 and T_4 become too high, then D3 is recruited from the plasma membrane [22], and, together with D1, it converts T_3 and T_4 into the inactive metabolites rT_3 (reverse T_3) and T_2 (3,3′-diiodothyronine) respectively. Levels of D3 are T_3-dependent, requiring the presence of TR (TH receptor) α [23]; this feedback mechanism is vital for the control of both the hypothalamic–pituitary–thyroid axis [24,25] and TH levels throughout the body.

Dio3 shows particularly high expression in fetal and placental tissues [26,27], where it functions to protect the fetus from high levels of maternal TH. The majority of adult tissues demonstrate only low expression of *Dio3*; however, studies show that the rat brain maintains high D3 activity throughout life [28]. These data supports a functionally protective role for the enzyme, in this instance in modulating thyroid levels within neurons. In addition, in some circumstances, there is re-expression of *Dio3* in the adult, for example during proliferation and cell growth [29]. This has been demonstrated in a number of pathophysiological conditions including cancer, myocardial infarction and liver regeneration following partial hepatectomy [19,30,31].

Although much is known about the transcriptional regulation of *Dio3*, its translational, or post-transcriptional, regulation has not been extensively investigated. Levels of *Dio3* are increased transcriptionally in the presence of THs [32], retinoic acid [33] and growth factors [34], and reduced by growth hormones [35] and in hypothyroidism. Genomic imprinting of *Dio3*, via differentially methylated regions [36], is also suggested to be a contributor to transcriptional regulation [32]. Although not yet identified in the case of *Dio3*, there are published data on the other deiodinases that suggest that post-transcriptional regulation is essential; for example, *Dio2* demonstrates significant post-transcriptional regulation [37]. Within the brain, the translational regulation of *Dio2* is critical for the preservation of TH levels to prevent hypothyroidism, and it has been shown that the increases in D2 activity are far greater than can be accounted for by transcriptional changes in *Dio2* mRNA [38]. Within the rat and human adult liver, *Dio2* is not expressed [39]; however, *Dio3* is. We therefore investigated whether within the liver this important mode of regulation could be controlled by *Dio3* rather than *Dio2*.

In the present study, we show that *Dio3*, like *Dio2*, can show a change in expression at the post-transcriptional level. We hypothesize that this mechanism may play a key role in the synthesis of D3 protein, the control of TH levels and the maintenance of the hypothalamic–pituitary– thyroid axis in cases of drug-induced cellular stress to the liver.

EXPERIMENTAL

Animals: PredTox

With a view to reducing the financial and time restraints caused by the extensive testing required for any new drug candidate, a consortium comprising 15 pharmaceutical companies, two SMEs (small and medium enterprises) and three universities was set up in 2005. This consortium, the InnoMed PredTox project, formed under European Union Framework Programme 6, sought to develop genomic biomarkers for the early detection of drug-induced toxicity. Male Wistar rats received pharmacologically active doses of 14 compounds that had failed in development owing to hepato- and/or nephro-toxicity. The treatment regime involved dosing for up to 15 days with a vehicle dose, a low dose or a high dose of each compound. The five agents that caused the most pronounced hepatobiliary injury were selected for further investigation in the present study. Liver samples from rats treated with these five compounds were provided as donations from the PredTox consortium. The compounds and their properties are shown in Supplementary Table S1 at http://www.biochemj.org/bj/453/bj4530071add.htm.

Animals: thioacetamide model

Male Wistar rats (3 months, 300–350 g) were dosed via the i.p. (intraperitoneal) route with Thioacetamide (Sigma) dissolved in 0.9 % saline to final doses of 50 mg/kg, 100 mg/kg and 150 mg/kg. These doses fall below the threshold for overt toxicity [12,13]. Vehicle-only-treated rats were used as controls. Six animals were used at each dose level and all Figures show means ± S.E.M. for each measurement. After 24 h, half of the animals from each group were anaesthetized using isoflurane and blood was withdrawn via the descending vena cava. Blood was collected into lithium/heparin tubes and the plasma was isolated. Organs were perfused *in situ* with PBS and animals were killed by decapitation under terminal anaesthesia. Organs were harvested, sections were taken for histological analysis and the remainder were snap-frozen in liquid nitrogen. The remaining animals from each group underwent the same process after a further 24 h. All procedures were licensed under U.K. Home Office project licence 80/2126.

Measurement of ALT (alanine transaminase) and AST (aspartate aminotransferase) levels

To measure plasma levels of ALT and AST, kits from Sentinel Diagnostics (Alpha Laboratories) were used according to the manufacturer's instructions.

Translational profiling

Sucrose density fractionation was used to separate mRNAs according to their ribosomal mass. mRNAs that are under active translation will have a large number of ribosomes attached [40], increasing their density and resulting in them migrating towards the bottom of the gradient; those that are less actively translated, with fewer ribosomes attached, will be less dense and will therefore be situated towards the top of the gradient. Approximately 150 mg of each liver sample was ground to a powder in liquid nitrogen using a pestle and mortar and then lysed in 15 mM Tris/HCl (pH 8.0), 300 mM NaCl and 15 mM $MgCl_2$, plus inhibitors [1 mg/ml heparin, 100 μg/ml cycloheximide and 80 units of RNasin® (Promega)]. Following centrifugation at 12000 g for 5 min at 4°C, the resulting supernatant was added to a 10–50 % sucrose gradient and ultracentrifuged at 388000 rev./min in a Beckman ultracentrifuge for 2 h using a SW40 rotor. Sucrose of a greater density was used in combination with a Harvard syringe pump system to divide each gradient into ten to 16 individual 1 ml fractions. These fractions were collected
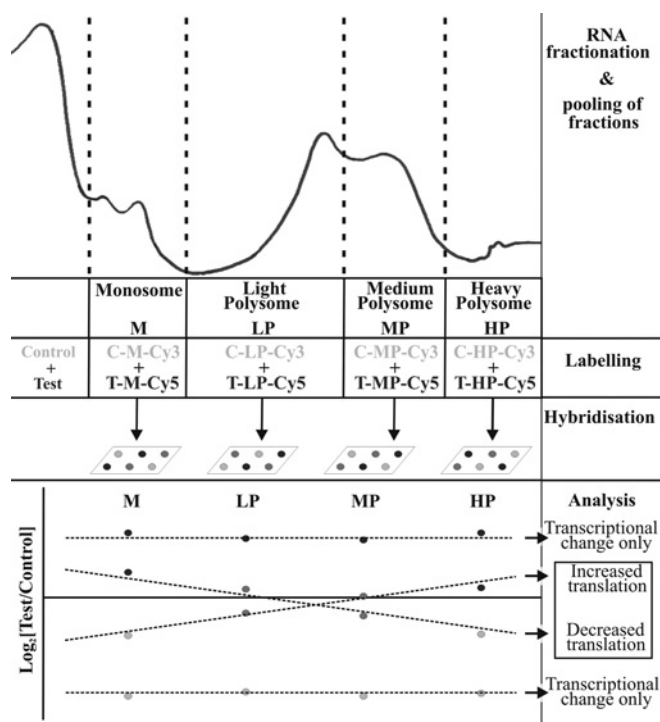
Figure 1   Translational profiling of liver samples taken from rats treated with the PredTox compound FP014SC

RNA from the livers of control (vehicle-treated) and test (compound-treated) animals was fractionated by sucrose density centrifugation and pooled into four fractions: monosome (M), light polysome (LP), medium polysome (MP), and heavy polysome (HP). Each of the four control (C) fractions were labelled with Cy3 and hybridized against each of the four corresponding test (T) fractions labelled with Cy5. The statistical significance of differences between C and T in each of the four fractions was calculated using a reverse-labelled two-tailed Student's *t* test [41]. All data with four *P* values >0.05 were rejected. Linear regression analysis was then performed on the four log$_2$ ratios of test fractions/control fractions. This showed movement of mRNAs through the gradient and enabled differentially translated mRNAs to be identified. Reverse-labelling reactions were also performed and incorporated into the analysis.

into tubes containing 1 ml of Tri Reagent (Sigma), and RNA was extracted according to the manufacturer's instructions.

Genomic analysis of mRNA fractions

The individual fractions were subpooled into four groups, monosomal, light polysomal, medium polysomal and heavy polysomal (Figure 1), according to ribosomal density. Microarray analysis was performed by hybridizing control (vehicle-treated) monosomes against test (high-dose-treated) monosomes on one microarray, control light polysomes against test light polysomes on a second microarray, and so forth for each subpool of fractions (Figure 1). Equal amounts of RNA from each subpool were precipitated with 10 μl of 3 M sodium acetate (pH 5.2) and 275 μl of 100 % ethanol at −20°C overnight. Following centrifugation at 12000 *g* for 10 min at 4°C, pellets were washed twice with 75 % ethanol and resuspended in 10 μl of water. The precipitated RNA was reverse-transcribed, hydrolysed and coupled to a dUTP-conjugated Cy3 (indocarbocyanine) or Cy5 (indodicarbocyanine) dye (GE Healthcare). The labelled cDNA samples were mixed and hybridized at 42°C overnight to a 70-mer MEEBO (Mouse Exonic Evidence-Based Oligonucleotide) microarray (http://www.microarray.org/sfgf/meebo.do). The microarrays were printed in-house using an ArrayJet Ultra Marathon microarrayer and an Illumina probe set (Invitrogen), which covers the

entire mouse genome. We had established previously that these microarrays showed excellent cross-species reactivity between mouse and rat (T. Gant, unpublished work). Following overnight incubation, the slides were washed [wash 1: 1× SSC (1× SSC is 0.15 M NaCl/0.015 M sodium citrate) and 0.03 % SDS for 5 min; wash 2: 0.2× SSC for 3 min; and wash 3: 0.05× SSC for 3 min] and scanned on a 4200A Axon scanner (Molecular Devices). Experiments were performed in duplicate, incorporating a dye-swap technique for $n = 5$ pairs of samples. Once all hybridization reactions were complete, the results were normalized by LOWESS (locally weighted scatterplot smoothing), which uses locally weighted regression to smooth scattered data (S. Zhang, personal communication) and tested for statistical significance using a two-tailed Student's *t* test as described previously [41]. There were a maximum of four values for each mRNA, corresponding to the proportional representation of it within each subpool of fractions. By calculating the change in values, i.e. degree of slope, across the monosomal, light polysomal, medium polysomal and dense polysomal region, it was possible to determine any translational shift. In addition, the overall change in transcriptional activity across the gradient was calculated for each mRNA. The full dataset has been submitted to GEO (Gene Expression Omnibus) under accession number GSE38807. Pathway analysis of differentially translated mRNAs was performed using Ingenuity IPA software.

Western blotting

Tissue samples were lysed at 4°C in lysis buffer [50 mM Tris/HCl (pH 7.4), 150 mM NaCl, 5 mM EDTA, 1 % Nonidet P40, 0.25 % sodium deoxycholate and protease inhibitors]. Protein (30 μg) was separated on a 10 % acrylamide gel and transferred on to a nitrocellulose membrane (GE Healthcare). Membranes were blocked with 10 % (w/v) Marvel non-fat dried skimmed milk powder in TBST (Tris-buffered saline with 0.05 % Tween 20) and incubated at 4°C overnight with the primary antibody anti-Dio3 (1:1000 dilution) (Novus Biologicals) in 5 % Marvel. This antibody has previously been validated [42,43] against the only other available anti-D3 antibody [44]. Following overnight incubation and washing in TBST, membranes were incubated with the appropriate horseradish peroxidase-conjugated anti-rabbit secondary antibody (1:1000 dilution), (Santa Cruz Biotechnology) and visualized using ECL (enhanced chemiluminescence) Western blotting detection reagents (GE Healthcare). To check for equal loading, membranes were stripped using 62.5 mM Tris/HCl (pH 6.8), 2 % (w/v) SDS and 100 mM 2-mercaptoethanol, re-blocked and incubated overnight with anti-GAPDH (glyceraldehyde-3-phosphate dehydrogenase) (1:30000 dilution) (Sigma). Western blots were quantified using the gel analysis function of ImageJ software (NIH). To analyse time-course and dose–response effects, one-way ANOVA with Tukey's multiple comparison post-hoc test was performed using GraphPad Prism (version 5.01). Results are expressed as means ± S.E.M. $P < 0.05$ was considered significant.

RNA isolation and qRT-PCR (quantitative reverse transcription–PCR)

RNA was extracted from <100 mg of liver samples using Tri Reagent according to the manufacturer's guidelines. RNA quality was assessed using an Agilent Bioanalyser, where a RIN (RNA integrity number) score of >8.5 was used as an indication that RNA was of a suitable quality for further work. To prevent genomic DNA contamination, 10 μg of RNA was

Table 1   Summary of the histopathological data for each of the PredTox compounds

Severity levels: +++>++>+.

Framework Programme 6 study name	Compound sponsor	Toxicological response within liver	Severity
FP004BA	Bayer	Bile duct damage Hepatocyte necrosis Regenerative hyperplasia Inflammatory responses Cholestasis Fibrosis	++
FP005ME	Merck	Hepatocellular apoptosis Necrosis Peribiliary inflammation Fibrosis Bile duct proliferation and necrosis Hepatocellular hypertrophy	+
FP007SE	Boehringer Ingelheim	Increased transamininases, ALP and bilirubin Pericholangitis with bile duct hyperplasia Cholestasis Inflammation Hepatocellular hypertrophy Vacuolation	++
FP013NO	Novartis	Absence of hepatocellular glycogen deposits Increased fatty deposits	+
FP014SC	Bayer Schering Pharma (formerly Schering)	Severe acute necrotic liver injury Elevated liver transaminases Cholestasis Hepatocellular vacuolation and hypertrophy Regeneration and increased mitosis	+++

treated with Turbo DNase (Applied Biosystems) according to the manufacturer's instructions. The DNase was inactivated through re-extraction of the RNA, as described above. RNA (1 μg) was reverse-transcribed using a high-capacity reverse transcription kit (Applied Biosystems) and then qRT-PCR was performed using an ABI Prism® 7000 Sequence Detection System. Primers against *Dio3* and *Actb* (β-actin) (housekeeping gene) were designed using Primer Express version 2.0.0 (Applied Biosystems) and ordered from Sigma–Aldrich. Primer sequences are given in Supplementary Table S2 at http://www.biochemj.org/bj/453/bj4530071add.htm. All primers were tested for percentage efficiency before use [45]. Reactions were performed in 25 μl of *Power* SYBR® Green PCR Master Mix (Applied Biosystems), using 450 nM each of forward and reverse primer.

Northern blot analysis

An equal volume of RNA from each fraction was loaded on to a denaturing agarose gel as described previously [46] and, following overnight electrophoresis, was transferred on to MagnaGraph nylon transfer membrane (Labtech International) by capillary transfer ($10\times$ SSC). The membrane was cross-linked with 120 mJ/cm^2 UV for 60 s. In addition, fractionated RNA was mixed with denaturing buffer [59 % (v/v) deionized formamide, 24 % (v/v) formaldehyde and 0.14 M Mops], dot-blotted on to the same membrane and cross-linked as described above. Probes derived from PCR products to the coding regions of *Dio3* and *Actb* (primer sequences given in Supplementary Table S2) were labelled with ^{32}P using *Escherichia coli* Klenow fragment, and incorporation was measured by scintillation counting. Probe (10^6 d.p.m./ml) was added to the pre-hybridized [50 % (v/v) deionized formamide, $6\times$ SSC, $5\times$ Denhardt's solution (0.1 % Ficoll 400/0.1 % polyvinylpyrrolidone/0.1 % BSA) and 1 % (w/v) SDS] membranes and hybridized for 48 h at 42 °C. The hybridized membranes were visualized using autoradiography and quantified

using ImageQuant TL (version 2003.03). The value for each gradient fraction was expressed as a percentage of the total for the whole gradient.

Determination of T_3 and T_4 concentrations

The levels of T_3 and T_4 in the liver and plasma were determined by highly sensitive and specific RIAs, as described in detail in [47,48].

RESULTS

Assessment of liver damage

Previous work by the PredTox consortium indicated that the five compounds selected for further analysis in the present study caused hepatic injury, as determined by histopathology and clinical chemistry (Table 1). We supplemented the PredTox model with the thioacetamide-treated rat model. To determine the degree of liver injury in this additional model, plasma ALT and AST levels were measured 24 h after administration of 100 mg/kg thioacetamide. Enzyme levels were increased more than 10 (ALT) and 43 (AST) -fold when compared with the vehicle-treated samples (Figure 2A). Levels of both enzymes in the treated animals were lower at 48 h than at 24 h, reflecting the acute nature of the hepatic injury and subsequent initiation of repair mechanisms.

Clinical chemistry data were supported by histopathological analysis. Representative images from the livers of rats treated with the vehicle and the highest dose (150 mg/kg) of thioacetamide are shown in Figure 2(B). The images from the treated livers demonstrated some fibrosis and inflammation; the hepatocytes had small dense nuclei, indicative of hepatic injury, and there was also evidence of hepatocyte vacuolation (Figure 2B, indicated by V). However, there were also signs of some regeneration
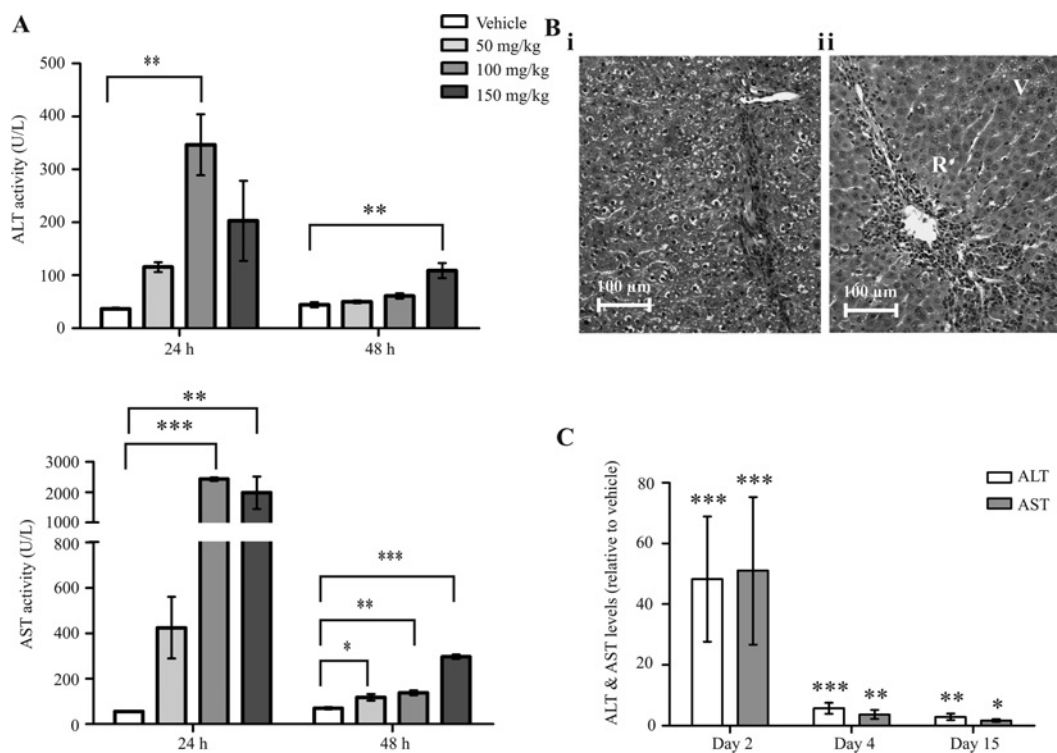
Figure 2 Clinical chemistry and histopathology indicate hepatotoxicity following treatment with thioacetamide and the PredTox compounds

(**A**) Plasma ALT and AST levels (in units/litre) and (**B**) histopathological images 48 h after treatment with (i) vehicle-only and (ii) 150 mg/kg thioacetamide. V, vacuolation, indicative of hepatocellular injury; R, area rich in hepatocytes forming parenchymal nodules, indicative of enhanced regenerative activity. (**C**) ALT and AST levels relative to control animals from the plasma of rats treated with the PredTox compound FP014SC. Results are means $\pm$ S.E.M. ($n = 3$). *$P \leqslant 0.05$, **$P \leqslant 0.01$, ***$P \leqslant 0.001$ (ANOVA with Dunnett's post-hoc test to compare groups).

(Figure 2B, indicated by R) after 48 h, concurrent with the decreased levels of serum transaminases.

ALT and AST levels were similarly increased following treatment with the PredTox compounds. Representative data from the most severe hepatotoxic agent (FP014SC) is given in Figure 2(C). As with the thioacetamide, this effect was transient and levels had returned to close to those seen in the vehicle-treated samples by 15 days after treatment.

The histopathological summary for each of the PredTox compounds indicated a histology similar to that seen in the livers of the thioacetamide-treated rats, with common features including apoptosis, inflammation, cholestasis and regenerative repair (Table 1).

Microarray analysis indicated that D3 is involved in drug-induced hepatotoxicity

Translational microarray analysis was performed on RNA from those PredTox samples treated with the most potent hepatotoxic agent, FP014SC (Table 1), at the highest dose and latest time point (1120 mg/kg, day 15). Analysis of polysome-associated mRNAs showed an alteration in the numbers of ribosomes recruited to individual mRNAs, indicative of changes in translational efficiency. All mRNAs that demonstrated a shift in ribosomal occupancy across the gradient (Supplementary Table S3 at http://www.biochemj.org/bj/453/bj4530071add.htm) were subjected to pathway analysis using IPA software. From this analysis, 169 canonical pathways were identified as having two or more altered genes (Supplementary Table S4 at http://www.biochemj.org/bj/453/bj4530071add.htm). Pathways under the control of RXR (retinoid X receptor) were highlighted because RXR plays

a fundamental role in many disrupted metabolic pathways. Individual examination of RXR-based canonical pathways identified *Dio3* as an indirect regulator of RXR, via the control it exerts over TH levels. This is demonstrated in the TR/RXR activation pathway (Figure 3); other related canonical pathways (indicated by CP) are also highlighted. *Dio3* displayed a shift from the heavy polysomal region, to the lighter monosomal region following treatment with FP014SC (Supplementary Table S3), reflecting decreased ribosomal occupancy. This indicated that *Dio3* was less actively translated following treatment with FP014SC.

D3 is down-regulated following drug-induced hepatotoxicity

Reduced translational efficiency of an mRNA should cause a corresponding decrease in protein levels. We carried out Western blot analysis to determine D3 levels in the livers of rats treated with the PredTox compounds or thioacetamide. Following high-dose treatment for 15 days with FP004BA, FP007SE and FP014SC (Figures 4A–4C), there was a significant reduction in D3. In addition, high-dose treatment (150 mg/kg) with thioacetamide for 48 h (Figure 4D) caused significantly decreased D3 levels. A similar trend was seen with the other PredTox compounds, FP005ME and FP013NO (Figures 4E and 4F), although they failed to reach statistical significance. When considering samples on an individual basis, there was a correlation between the extent of liver damage, according to clinical and histopathological grading, and reduction in D3 levels. We therefore also tested whether dose- and time-course-related responses were evident. To measure time-related effects, we used the PredTox sample that had shown the largest reduction in
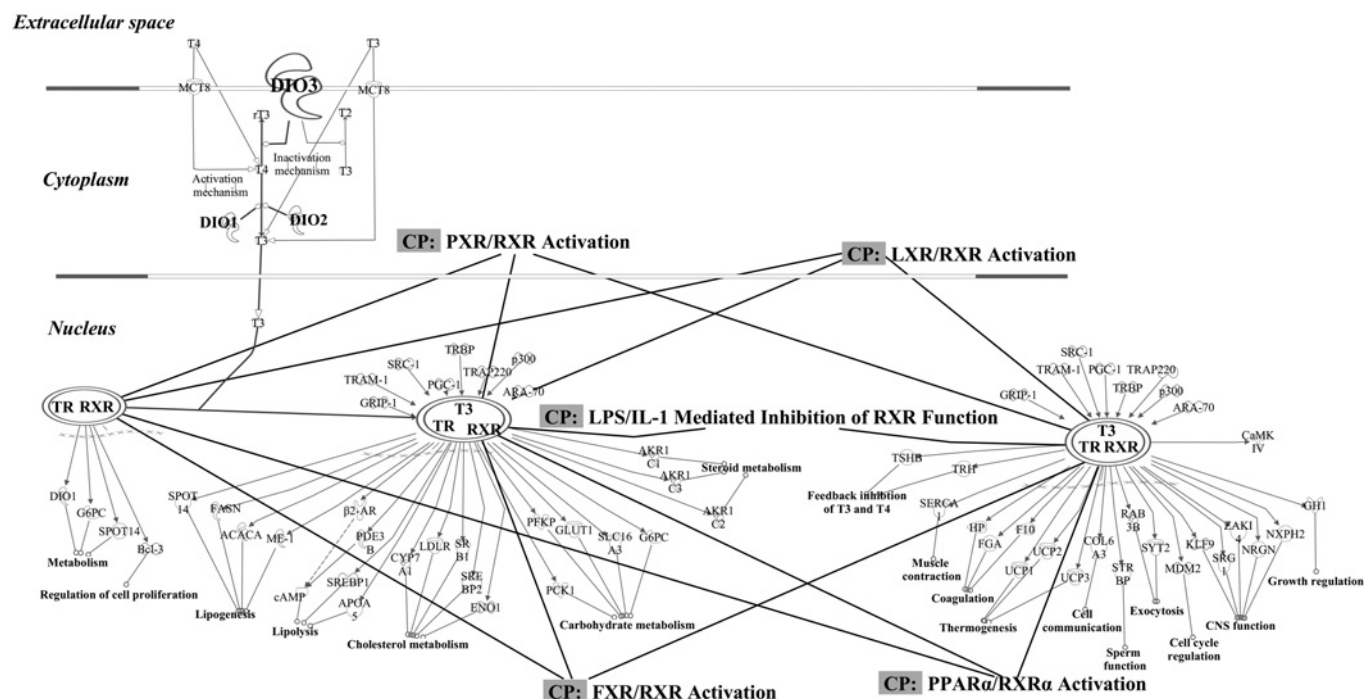
Figure 3   Networks of the TR/RXR activation pathway

All mRNAs that demonstrated a change in translational efficiency were subject to pathway analysis using Ingenuity® IPA software. TR/RXR was identified as a key pathway. Associated RXR canonical pathways are also highlighted ('CP'): FXR, farnesoid X receptor; IL-1, interleukin 1; LPS, lipopolysaccharide; LXR, liver X receptor; PPARα, peroxisome-proliferator-activated receptor α; PXR, pregnane X receptor. *Dio3* plays a regulatory role in the TR/RXR pathway via the control it exerts over thyroid levels.

D3 levels (FP007SE) following high-dose treatment for 15 days. The reduction in D3 was exacerbated over time, until, by day 15, levels were reduced to less than 15% of the vehicle-treated samples (Figure 5A). We used the thioacetamide model to look for a dose–response effect in the reduction of D3 with hepatotoxicity. Although the only statistically significant reduction in D3 was seen following treatment at the highest dose (150 mg/kg), there was a small, but consistent, change at the lower doses (Figure 5B). Two of the other PredTox compounds caused a similar effect (Supplementary Figure S1 at http://www.biochemj.org/bj/453/bj4530071add.htm).

The reduction in protein was not due to changes in the level of *Dio3* mRNA

To confirm that changes in D3 at the protein level were occurring independently of a change in transcriptional activity, we performed qRT-PCR on total RNA. This showed either no change in *Dio3* mRNA levels or, in the case of FP007SE, a statistically significant increase in *Dio3* mRNA levels (Figure 6A). High-dose thioacetamide treatment caused a non-significant increase 48 h after dosing (Figure 6B) and the other PredTox compounds resulted in no change in *Dio3* mRNA levels (Supplementary Figure S2 at http://www.biochemj.org/bj/453/bj4530071add.htm).

Less D3 was recruited to the polysomes following drug-induced hepatotoxicity

Using the FP007SE and thioacetamide studies, we performed Northern blot analysis to verify that changes were occurring post-

transcriptionally, at the translational level. Hybridizing with a radiolabelled probe enabled the proportional representation of *Dio3* across the density gradient to be determined. We saw an increase in *Dio3* mRNA abundance in the lighter fractions of the compound-treated samples compared with the vehicle-treated samples (Figures 6C, i, and 6D, i), indicating lower translational efficiency. A similar validation technique was performed by machine dot-blotting RNA from each fraction across the gradient on to a nylon membrane and hybridization with the same *Dio3*-specific probe. As with the initial Northern blot analysis, when quantified, the treated samples demonstrated a shift from the heavier density fractions to the lighter density fractions (Figure 6C, ii, and 6D, ii). This supported the hypothesis that the changes in protein levels were due to fewer ribosomes being recruited and therefore less efficient translation of *Dio3* mRNA.

The liver and plasma had reduced levels of T_3 and T_4 following toxic injury

We measured levels of T_3 and T_4 within the liver following treatment with FP007SE or thioacetamide. We saw that, following treatment with FP007SE for 15 days, there was a reduction in levels of both hormones: by 57% (T_3) and 53% (T_4) (Figure 7A). Similarly, thioacetamide caused a reduction in T_3 and T_4 levels by 73% and 25% respectively 24 h after dosing (Figure 7B, i). The levels of T_4 were also reduced in two of the other PredTox studies (Supplementary Figure S3 at http://www.biochemj.org/bj/453/bj4530071add.htm). We also measured the levels of T_3 and T_4 in the plasma of the thioacetamide-treated rats. T_3 levels were reduced by up to 60% 24 h after dosing. Although statistical significance was not achieved, T_4 levels also showed a trend for
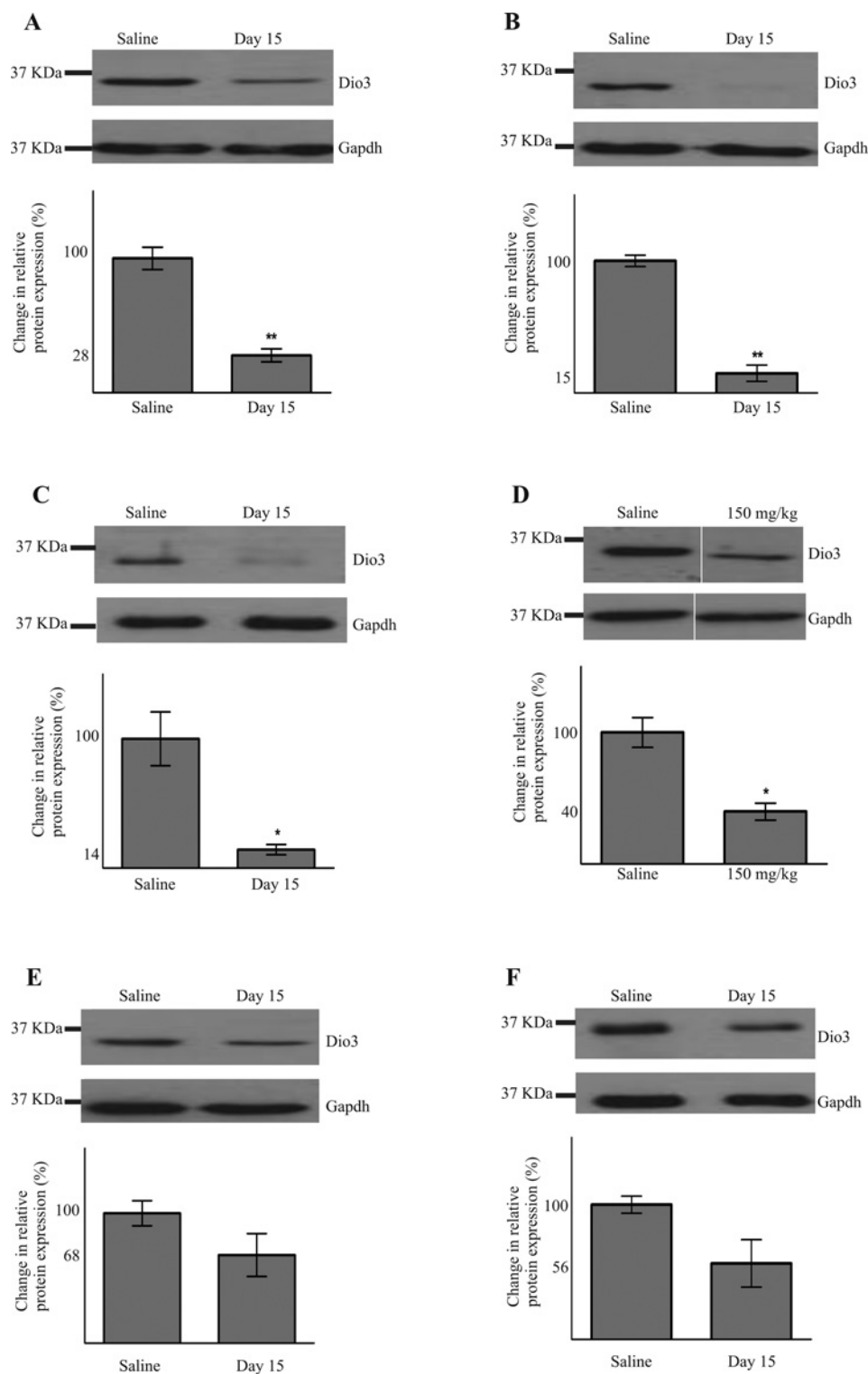
Figure 4   D3 protein is down-regulated following drug-induced liver damage

Western blot analysis was performed on lysates from the livers of rats treated at high-dose levels with various hepatotoxic agents. D3 protein levels were normalized to those of GAPDH. Representative gel images are shown for PredTox compounds FP004BA (**A**), FP007SE (**B**), FP014SC (**C**) and thioacetamide (**D**). Non-significant reductions were seen with PredTox compounds FP005ME (**E**) and FP013NO (**F**). Mean relative levels of D3 are indicated beneath each gel image. The position of a 37 kDa protein is indicated. Results are means ± S.E.M. ($n \geqslant 3$). *$P \leqslant 0.05$, **$P \leqslant 0.001$ (Student's *t* test).

a reduction following treatment (Figure 7B, ii). T_4 has a long half-life in the plasma and therefore the concentration of this enzyme within the systemic circulation usually remains relatively stable [20]. Sample availability from the PredTox studies was limited, and did not allow measurement of T_3 and T_4 levels in the plasma.
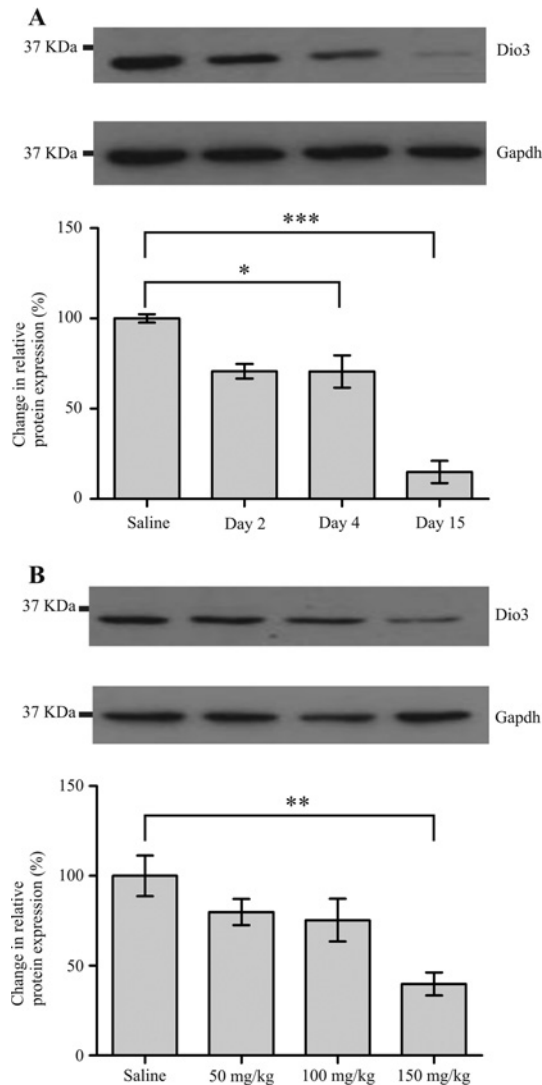
Figure 5   D3 protein is down-regulated in both a time- and dose-dependent manner

Western blot analysis was performed on lysates from the livers of rats treated with various hepatotoxic agents. D3 protein levels were normalized to those of GAPDH. Representative gel images are shown for (**A**) PredTox compound FP007SE and (**B**) thioacetamide. Mean relative levels of D3 are indicated beneath each gel image. The position of a 37 kDa protein is indicated. Results are means $\pm$ S.E.M. ($n = 3$). *$P \leqslant 0.05$, **$P \leqslant 0.01$, ***$P \leqslant 0.001$ (ANOVA with Dunnett's post-hoc test to compare groups).

DISCUSSION

In the present study, we used global genomic methods to investigate changes in the rate of translation of thousands of individual mRNAs concurrently in two models of drug-induced hepatotoxicity. A change in the rate of mRNA translation can bring about a rapid efficient change in protein levels, without the need to generate more transcript [3]. We identified *Dio3* as an mRNA showing a reduction in the rate of translational activity following hepatotoxicity. The present study provides evidence that the translational repression of *Dio3* results in less D3 protein, independent of any change in mRNA level, and suggests that the reduced translation is a regulatory mechanism, enabling the liver to combat cellular stress. The known function of *Dio3* in modulating thyroxine levels supports further the hypothesis

that post-transcriptional regulation may be a rapid compensatory response to drug-induced damage.

In the rat, D3 activity is reduced in cases of hypothyroidism [28,49], although the extent of the change varies between tissues [20]. The observed reductions in T_3 and T_4, along with the transcriptional down-regulation of *Dio1* mRNA (Supplementary Figure S4 at http://www.biochemj.org/bj/453/bj4530071add.htm), which is known to be down-regulated in cases of hypothyroidism, indicated that the livers of the treated rats were in a hypothyroid state [17,50].

Previously, changes in D3 activity have been found to correlate strongly with changes in expression of *Dio3* mRNA [49]; however, we found no evidence for the change in protein production being regulated at a transcriptional level. Moreover, one of the PredTox compounds (FP007SE) showed a transcriptional increase in *Dio3* mRNA within the liver following high-dose treatment (Figure 6A). This was in agreement with previous studies on *Dio3*, where an increase in expression was investigated [29–31]. To our knowledge, all previous work on *Dio3* in the liver has focused on cases of enhanced cellular proliferation, either during growth and development in the fetus [26] or in the adult at times of cellular stress, such as during critical illness [29]. Previous studies have assumed that the adult liver contains low to negligible levels of *Dio3* mRNA [23,50] and that, to measure transcriptional changes, cellular proliferation must first be induced. The PredTox consortium reported that, following 15 days of treatment with the FP007SE compound, there were signs of liver recovery and regeneration [51]. Furthermore, 48 h after dosing with thioacetamide, there were clinical and histological signs of liver repair, which concurred with an increase in *Dio3* mRNA levels. Therefore the results of the present study support what is widely reported in the literature whereby, in cases of cellular proliferation, *Dio3* mRNA shows an increase in expression. However, despite this increase we saw an almost total abolition of conversion of the mRNA into protein. We therefore hypothesized that the changes in protein levels were mediated predominantly by altered *Dio3* translation.

It is well established that another of the deiodinase genes, *Dio2*, is regulated at levels distinct from transcription and that these alter the levels of D2 expression independently of changes in mRNA level [37,52]. The change in activity of D2 is often greater than the change in *Dio2* mRNA, for example in brown adipose tissue following cold exposure [53] and the brain following experimentally induced hypo- and hyper-thyroidism [54]. This is essential for homoeostasis of the THs. Certainly, in cases of endoplasmic reticulum stress, D2 activity is reduced independently of transcriptional changes and this leads to a rapid, but significant, decrease in the levels of T_3 [37].

Taken in combination, the post-transcriptional control of D2 is therefore of critical importance in maintaining TH levels in mammals. However, within the rat and human liver, D2 is not expressed [20], and, as a result, an alternative method of regulation is necessary. We hypothesize that, following hepatotoxicity, D3 is recruited for TH homoeostasis in the liver. This seleno-enzyme functions primarily to inactivate T_3 and T_4 by conversion into their inactive metabolites, rT_3 and T_2 respectively [20]. As an inactivating enzyme, D3 acts primarily to protect tissues from an excess of TH. If this mechanism is disrupted in some way, severe hypothyroidism [19] or hyperthyroidism can occur.

We propose a mechanism whereby the hepatotoxins used in the present study have led to a need for increased energy for cellular proliferation, as part of the inflammatory response within the liver following cell damage. This is achieved through a rapid decrease in *Dio3* translation and consequent reduction in the level of D3 protein. Although we cannot rule out a role for increased protein degradation, the reduced ribosomal association of *Dio3*
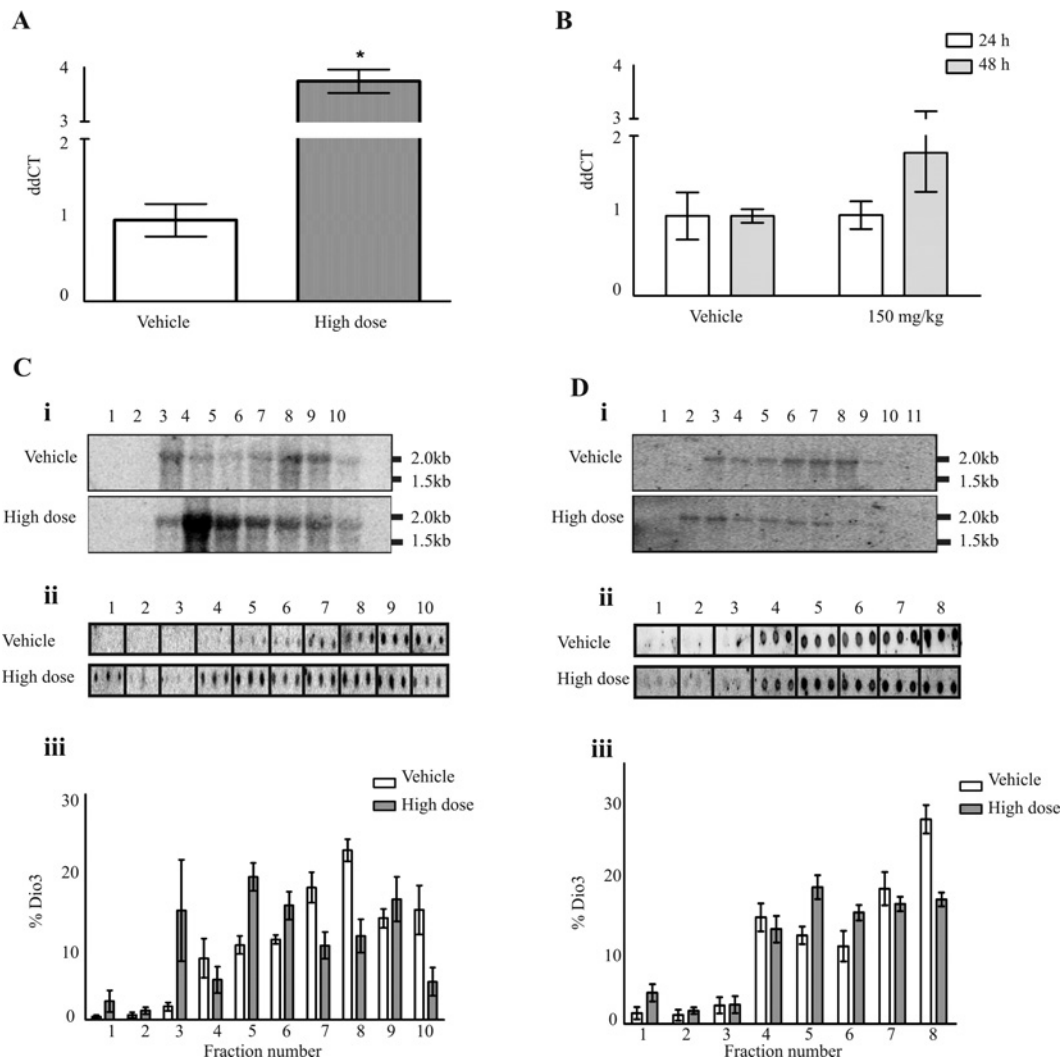
Figure 6   The reduction in D3 protein is due to changes in mRNA translation not transcription

qRT-PCR analysis was performed on RNA extracted from the livers of rats treated with high doses of (**A**) PredTox compound FP007SE for 15 days or (**B**) thioacetamide. Results are means $\pm$ S.E.M. ($n = 3$). $*P \leqslant 0.001$ (Student's t test). Polysomal association of *Dio3* was measured by Northern blot analysis. Liver samples from rats treated with high doses of either (**C**) FP007SE (15 days) or (**D**) thioacetamide (48 h) were lysed and fractionated using a 10–50 % sucrose gradient. RNA was extracted from individual fractions and electrophoresed on a denaturing agarose gel, before being transferred on to a nylon membrane (i). Sizes are indicated in kb. RNA from each fraction was also dot-blotted on to a nylon membrane (ii). All membranes were probed with a ^{32}P labelled probe specific to *Dio3*. The proportional representation of *Dio3* within each fraction was calculated. Representative images are shown for both compounds and results are the mean $\pm$ S.E.M. ($n = 3$) amount of *Dio3* within each fraction as a percentage of the total (iii).

mRNA shown experimentally in the present study in both model systems provides a strong case for translational repression being an important mechanism leading to the reduction in D3 protein. In cases where *Dio3* transcription is significantly up-regulated, as seen in Figure 6, in addition to a reduction in mRNA translation, protein degradation could also contribute to the reduced D3 protein levels.

The benefit of targeting *Dio3* post-transcriptionally is that the required response is efficient and rapid. A reduction in protein levels means less of the inactive metabolites rT_3 and T_2 are produced and alterations in T_3 and T_4 levels can be restored to normal (Figure 8). This is vital for maintaining the hypothalamic–pituitary–thyroid axis and means that all control is carried out at the local level, in concordance with the current literature [55]. As the liver regenerates and clinical signs of damage are reversed, protein levels are reduced further. This is probably for the required homoeostasis as the liver expends sufficient energy into tissue repair.

Although the levels of T_3 and T_4 within tissues are largely independent of those seen in the plasma [56], and the expression of the deiodinases is generally under localized regulation, the activity rate of the three deiodinases does directly affect the levels of circulating T_3 and T_4. This enables the feedback loop between the systemic organs and the thyroid gland to be maintained and has been experimentally validated in the case of D2, as described previously [37]. In the present study, we have demonstrated that, following treatment with thioacetamide, a known inducer of hypothyroidism, the levels of T_3 and T_4 were reduced in the plasma. The pattern of this change matched the changes in THs seen in the livers of treated animals (Figure 7B), although, as predicted by the literature [20], the change in T_4 was smaller. D3 is located within the plasma membrane, although the bulk of the molecule is extracellular [22]. This gives it ready access to, and control over, the levels of circulating THs. We propose that, because the liver is in rapid equilibrium with the plasma, it detects a change in THs and acts rapidly to prevent further production of
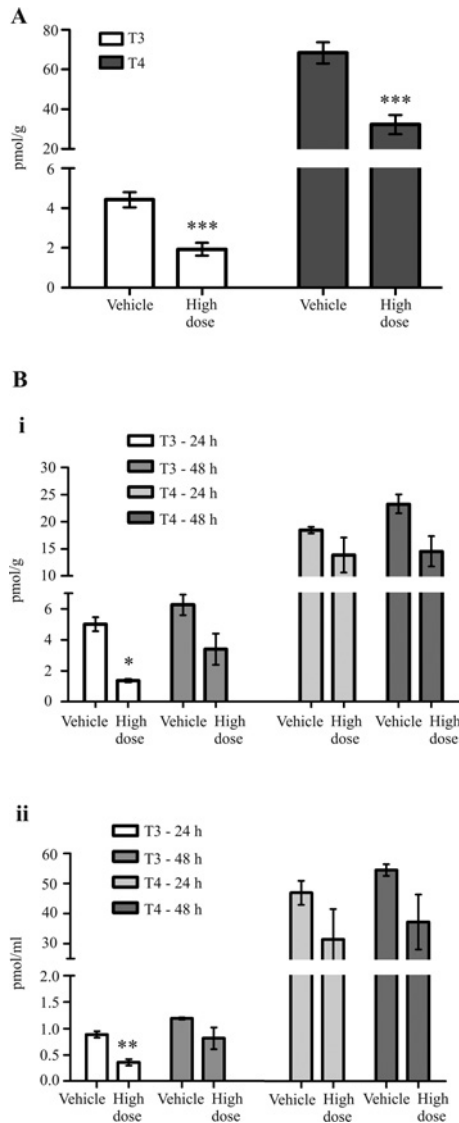
Figure 7   T$_3$ and T$_4$ levels within the liver and plasma are reduced following drug-induced liver damage

Liver samples were taken for measurement using highly sensitive and specific RIAs [47,48] following high-dose treatment with (**A**) PredTox compound FP007SE and (**B**, i) thioacetamide. (**B**, ii) Plasma samples were taken for measurement as above following treatment with thioacetamide. Results are means $\pm$ S.E.M. ($n \geqslant 3$). $*P \leqslant 0.05$, $**P \leqslant 0.01$, $***P \leqslant 0.001$ (Student's t test).

inactive metabolites (Figure 8). Through negative feedback, this mechanism enables levels of T$_3$ and T$_4$ in the liver to return to normal and ultimately restores homoeostasis within the liver.

Despite it being over 15 years since *Dio3* was first cloned [57], the regulation of this gene is complex and not yet fully understood. The gene is imprinted and preferentially expressed from the paternal allele [58]. In the mouse and humans, a non-coding gene transcribed in the antisense orientation, *Dio3os*, has been identified [59]; and very recent work indicates that a homologue of this gene may also be present in the rat [60]. *Dio3os* is proposed to belong to the family of lncRNAs (long non-coding RNAs), which, although commonly found in the mammalian genome, are poorly understood [61]. It has long been known that the stability of TRs can be moderated by naturally occurring antisense RNAs [62] and now that lncRNAs have been shown to directly regulate ribosomal association of their coding equivalent mRNAs [63], there is the distinct possibility that *Dio3* is post-transcriptionally regulated in this manner. In addition to this in the better characterized mouse and human orthologues, *Dio3os* and *Dio3* are partially overlapping and demonstrate inverse correlation of expression [59].

We conclude that the reduction in D3 expression levels during hepatotoxicity can be correlated with a change in *Dio3* mRNA translation rates. We hypothesize that this is an example of post-transcriptional control, which may be regulated by an lncRNA, *Dio3os*. We demonstrate that the magnitude of the decrease in protein is directly proportional to the extent of liver damage. This is probably due to the energy demand required for active repair processes to be initiated. TH homoeostasis has already been shown to play a role in a range of pathophysiological conditions and the results of the present study suggest that the pathway is also perturbed by drug-induced hepatotoxicity. We are able to provide evidence that this forms part of a rapid response by the liver and speculate that this occurs so that the initiation of a localized event remains consigned to the liver and does not affect the whole of the hypothalamic–pituitary–thyroid axis.

AUTHOR CONTRIBUTION

Kate Dudek, Timothy Gant and Emma Marczylo conceived and designed experiments. Kate Dudek, Veerle Darras and Laura Suter performed experiments and provided samples. Kate Dudek, Emma Marczylo and Timothy Gant wrote the paper.

ACKNOWLEDGEMENTS

Figure 8   Proposed mechanism of action following drug-induced hepatotoxicity

Steps in bold type are those experimentally demonstrated in the course of the present study. Non-bold type is used for the hypothesized mechanism of action and closure of the feedback loop. During hepatotoxicity, the liver is in a hypothyroid state and both the plasma and liver have reduced levels of T$_3$ and T$_4$. Consequently, the expression of D3 protein is reduced so that fewer inactive metabolites of T$_3$ and T$_4$ are produced and levels of both can return to normal, both locally (liver) and via plasma signals systemically.

REFERENCES

1 Sonenberg, N. and Hinnebusch, A. G. (2009) Regulation of translation initiation in eukaryotes: mechanisms and biological targets. Cell **136**, 731–745

2 Bottley, A., Phillips, N. M., Webb, T. E., Willis, A. E. and Spriggs, K. A. (2010) eIF4A inhibition allows translational regulation of mRNAs encoding proteins involved in Alzheimer's disease. PLoS ONE **5**, e13030

3 Le Quesne, J. P., Spriggs, K. A., Bushell, M. and Willis, A. E. (2010) Dysregulation of protein synthesis and disease. J. Pathol. **220**, 140–151

4 Spriggs, K. A., Bushell, M. and Willis, A. E. (2010) Translational regulation of gene expression during conditions of cell stress. Mol. Cell **40**, 228–237

5 Arava, Y., Wang, Y., Storey, J. D., Liu, C. L., Brown, P. O. and Herschlag, D. (2003) Genome-wide analysis of mRNA translation profiles in *Saccharomyces cerevisiae*. Proc. Natl. Acad. Sci. U.S.A. **100**, 3889–3894

6 Davidson, L. A., Wang, N., Ivanov, I., Goldsby, J., Lupton, J. R. and Chapkin, R. S. (2009) Identification of actively translated mRNA transcripts in a rat model of early-stage colon carcinogenesis. Cancer Prev. Res. **2**, 984–994

7 Kudo, K., Xi, Y., Wang, Y., Song, B., Chu, E., Ju, J. and Russo, J. J. (2010) Translational control analysis by translationally active RNA capture/microarray analysis (TrIP-Chip). Nucleic Acids Res. **38**, e104

8 Bartel, D. P. (2004) MicroRNAs: genomics, biogenesis, mechanism, and function. Cell **116**, 281–297

9 El Gazzar, M. and McCall, C. E. (2010) MicroRNAs distinguish translational from transcriptional silencing during endotoxin tolerance. J. Biol. Chem. **285**, 20940–20951

10 Greenman, I. C., Gomez, E., Moore, C. E. and Herbert, T. P. (2007) Distinct glucose-dependent stress responses revealed by translational profiling in pancreatic β-cells. J. Endocrinol. **192**, 179–187

11 Suter, L., Schroeder, S., Meyer, K., Gautier, J. C., Amberg, A., Wendt, M., Gmuender, H., Mally, A., Boitier, E., Ellinger-Ziegelbauer, H. et al. (2011) EU framework 6 project: predictive toxicology (PredTox): overview and outcome. Toxicol. Appl. Pharmacol. **252**, 73–84

12 Kucera, O., Lotkova, H., Stankova, P., Podhola, M., Rousar, T., Mezera, V. and Cervinkova, Z. (2011) Is rat liver affected by non-alcoholic steatosis more susceptible to the acute toxic effect of thioacetamide? Int. J. Exp. Pathol. **92**, 281–289

13 Mangipudy, R. S., Chanda, S. and Mehendale, H. M. (1995) Tissue repair response as a function of dose in thioacetamide hepatotoxicity. Environ. Health Perspect. **103**, 260–267

14 Hernandez, A., Garcia, B. and Obregon, M. J. (2007) Gene expression from the imprinted *Dio3* locus is associated with cell proliferation of cultured brown adipocytes. Endocrinology **148**, 3968–3976

15 Paternostro, M. A. and Meisami, E. (1994) Quantitative [³H]thymidine autoradiography of neurogenesis in the olfactory epithelium of developing normal, hypothyroid and hypothyroid-rehabilitated rats. Dev. Brain Res. **83**, 151–162

16 Simonides, W. S. and van Hardeveld, C. (2008) Thyroid hormone as a determinant of metabolic and contractile phenotype of skeletal muscle. Thyroid **18**, 205–216

17 Paquette, M. A., Dong, H., Gagne, R., Williams, A., Malowany, M., Wade, M. G. and Yauk, C. L. (2011) Thyroid hormone-regulated gene expression in juvenile mouse liver: identification of thyroid response elements using microarray profiling and *in silico* analyses. BMC Genomics **12**, 634

18 Dentice, M., Ambrosio, R. and Salvatore, D. (2009) Role of type 3 deiodinase in cancer. Expert Opin. Ther. Targets **13**, 1363–1373

19 Huang, S. A., Tu, H. M., Harney, J. W., Venihaki, M., Butte, A. J., Kozakewich, H. P., Fishman, S. J. and Larsen, P. R. (2000) Severe hypothyroidism caused by type 3 iodothyronine deiodinase in infantile hemangiomas. N. Engl. J. Med. **343**, 185–189

20 Bianco, A. C., Salvatore, D., Gereben, B., Berry, M. J. and Larsen, P. R. (2002) Biochemistry, cellular and molecular biology, and physiological roles of the iodothyronine selenodeiodinases. Endocr. Rev. **23**, 38–89

21 Bianco, A. C. (2011) Minireview: cracking the metabolic code for thyroid hormone signaling. Endocrinology **152**, 3306–3311

22 Baqui, M., Botero, D., Gereben, B., Curcio, C., Harney, J. W., Salvatore, D., Sorimachi, K., Larsen, P. R. and Bianco, A. C. (2003) Human type 3 iodothyronine selenodeiodinase is located in the plasma membrane and undergoes rapid internalization to endosomes. J. Biol. Chem. **278**, 1206–1211

23 Barca-Mayo, O., Liao, X. H., Alonso, M., Di Cosmo, C., Hernandez, A., Refetoff, S. and Weiss, R. E. (2011) Thyroid hormone receptor α and regulation of type 3 deiodinase. Mol. Endocrinol. **25**, 575–583

24 Hernandez, A., Martinez, M. E., Fiering, S., Galton, V. A. and St Germain, D. (2006) Type 3 deiodinase is critical for the maturation and function of the thyroid axis. J. Clin. Invest. **116**, 476–484

25 Boelen, A., Wiersinga, W. M. and Fliers, E. (2008) Fasting-induced changes in the hypothalamus–pituitary–thyroid axis. Thyroid **18**, 123–129

26 Bates, J. M., St Germain, D. L. and Galton, V. A. (1999) Expression profiles of the three iodothyronine deiodinases, D1, D2, and D3, in the developing rat. Endocrinology **140**, 844–851

27 Galton, V. A., Martinez, E., Hernandez, A., St Germain, E. A., Bates, J. M. and St Germain, D. L. (1999) Pregnant rat uterus expresses high levels of the type 3 iodothyronine deiodinase. J. Clin. Invest. **103**, 979–987

28 Kaplan, M. M. and Yaskoski, K. A. (1980) Phenolic and tyrosyl ring deiodination of iodothyronines in rat brain homogenates. J. Clin. Invest. **66**, 551–562

29 Peeters, R. P., Wouters, P. J., Kaptein, E., van Toor, H., Visser, T. J. and Van den Berghe, G. (2003) Reduced activation and increased inactivation of thyroid hormone in tissues of critically ill patients. J. Clin. Endocrinol. Metab. **88**, 3202–3211

30 Kester, M. H., Toussaint, M. J., Punt, C. A., Matondo, R., Aarnio, A. M., Darras, V. M., Everts, M. E., de Bruin, A. and Visser, T. J. (2009) Large induction of type III deiodinase expression after partial hepatectomy in the regenerating mouse and rat liver. Endocrinology **150**, 540–545

31 Wassen, F. W., Schiel, A. E., Kuiper, G. G., Kaptein, E., Bakker, O., Visser, T. J. and Simonides, W. S. (2002) Induction of thyroid hormone-degrading deiodinase in cardiac hypertrophy and failure. Endocrinology **143**, 2812–2815

32 Hernandez, A. (2005) Structure and function of the type 3 deiodinase gene. Thyroid **15**, 865–874

33 Esfandiari, A., Gagelin, C., Gavaret, J. M., Pavelka, S., Lennon, A. M., Pierre, M. and Courtin, F. (1994) Induction of type III-deiodinase activity in astroglial cells by retinoids. Glia **11**, 255–261

34 Hernandez, A., St Germain, D. L. and Obregon, M. J. (1998) Transcriptional activation of type III inner ring deiodinase by growth factors in cultured rat brown adipocytes. Endocrinology **139**, 634–639

35 Van der Geyten, S., Buys, N., Sanders, J. P., Decuypere, E., Visser, T. J., Kuhn, E. R. and Darras, V. M. (1999) Acute pretranslational regulation of type III iodothyronine deiodinase by growth hormone and dexamethasone in chicken embryos. Mol. Cell. Endocrinol. **147**, 49–56

36 Charalambous, M. and Hernandez, A. (2012) Genomic imprinting of the type 3 thyroid hormone deiodinase gene: regulation and developmental implications. Biochim. Biophys. Acta **7**, 3946–3955

37 Arrojo, E. D. R. and Bianco, A. C. (2011) Type 2 deiodinase at the crossroads of thyroid hormone action. Int. J. Biochem. Cell Biol. **43**, 1432–1441

38 Peeters, R., Fekete, C., Goncalves, C., Legradi, G., Tu, H. M., Harney, J. W., Bianco, A. C., Lechan, R. M. and Larsen, P. R. (2001) Regional physiological adaptation of the central nervous system deiodinases to iodine deficiency. Am. J. Physiol. Endocrinol. Metab. **281**, E54–E61

39 Croteau, W., Davey, J. C., Galton, V. A. and St Germain, D. L. (1996) Cloning of the mammalian type II iodothyronine deiodinase: a selenoprotein differentially expressed and regulated in human and rat brain and other tissues. J. Clin. Invest. **98**, 405–417

40 Hamilton, T. L., Stoneley, M., Spriggs, K. A. and Bushell, M. (2006) TOPs and their regulation. Biochem. Soc. Trans. **34**, 12–16

41 Zhang, S. D. and Gant, T. W. (2004) A statistical framework for the design of microarray experiments and effective detection of differential gene expression. Bioinformatics **20**, 2821–2828

42 Shukla, P. K., Sittig, L. J., Ullmann, T. M. and Redei, E. E. (2011) Candidate placental biomarkers for intrauterine alcohol exposure. Alcohol Clin. Exp. Res. **35**, 559–565

43 Sittig, L. J., Shukla, P. K., Herzing, L. B. and Redei, E. E. (2011) Strain-specific vulnerability to alcohol exposure *in utero* via hippocampal parent-of-origin expression of deiodinase-III. FASEB J. **25**, 2313–2324

44 Huang, S. A., Dorfman, D. M., Genest, D. R., Salvatore, D. and Larsen, P. R. (2003) Type 3 iodothyronine deiodinase is highly expressed in the human uteroplacental unit and in fetal epithelium. J. Clin. Endocrinol. Metab. **88**, 1384–1388

45 Bustin, S. A., Benes, V., Garson, J. A., Hellemans, J., Huggett, J., Kubista, M., Mueller, R., Nolan, T., Pfaffl, M. W., Shipley, G. L. et al. (2009) The MIQE guidelines: minimum information for publication of quantitative real-time PCR experiments. Clin. Chem. **55**, 611–622

46 Pointon, A. V., Walker, T. M., Phillips, K. M., Luo, J., Riley, J., Zhang, S. D., Parry, J. D., Lyon, J. J., Marczylo, E. L. and Gant, T. W. (2010) Doxorubicin *in vivo* rapidly alters expression and translation of myocardial electron transport chain genes, leads to ATP loss and caspase 3 activation. PLoS ONE **5**, e12733

47 Darras, V. M., Huybrechts, L. M., Berghman, L., Kuhn, E. R. and Decuypere, E. (1990) Ontogeny of the effect of purified chicken growth hormone on the liver 5′ monodeiodination activity in the chicken: reversal of the activity after hatching. Gen. Comp. Endocrinol. **77**, 212–220

48 Reyns, G. E., Janssens, K. A., Buyse, J., Kuhn, E. R. and Darras, V. M. (2002) Changes in thyroid hormone levels in chicken liver during fasting and refeeding. Comp. Biochem. Physiol., Part B: Biochem. Mol. Biol. **132**, 239–245

49 Mori, K., Yoshida, K., Fukazawa, H., Kiso, Y., Sayama, N., Kikuchi, K., Aizawa, Y. and Abe, K. (1995) Thyroid hormone regulates rat placental type III iodothyronine deiodinase activity by inducing kinetic changes different from those in the same isozyme in rat brain. Endocr. J. **42**, 753–760

50 Ng, L., Lyubarsky, A., Nikonov, S. S., Ma, M., Srinivas, M., Kefas, B., St Germain, D. L., Hernandez, A., Pugh, Jr, E. N. and Forrest, D. (2010) Type 3 deiodinase, a thyroid-hormone-inactivating enzyme, controls survival and maturation of cone photoreceptors. J. Neurosci. **30**, 3347–3357

51 Matheis, K. A., Com, E., Gautier, J. C., Guerreiro, N., Brandenburg, A., Gmuender, H., Sposny, A., Hewitt, P., Amberg, A., Boernsen, O. et al. (2011) Cross-study and cross-omics comparisons of three nephrotoxic compounds reveal mechanistic insights and new candidate biomarkers. Toxicol. Appl. Pharmacol. **252**, 112–122

52 Steinsapir, J., Harney, J. and Larsen, P. R. (1998) Type 2 iodothyronine deiodinase in rat pituitary tumor cells is inactivated in proteasomes. J. Clin. Invest. **102**, 1895–1899

53 Curcio-Morelli, C., Zavacki, A. M., Christofollete, M., Gereben, B., de Freitas, B. C., Harney, J. W., Li, Z., Wu, G. and Bianco, A. C. (2003) Deubiquitination of type 2 iodothyronine deiodinase by von Hippel–Lindau protein-interacting deubiquitinating enzymes regulates thyroid hormone activation. J. Clin. Invest. **112**, 189–196

54 Fekete, C., Freitas, B. C., Zeold, A., Wittmann, G., Kadar, A., Liposits, Z., Christoffolete, M. A., Singru, P., Lechan, R. M., Bianco, A. C. et al. (2007) Expression patterns of WSB-1 and USP-33 underlie cell-specific posttranslational control of type 2 deiodinase in the rat brain. Endocrinology **148**, 4865–4874

55 Gereben, B., Zeold, A., Dentice, M., Salvatore, D. and Bianco, A. C. (2008) Activation and inactivation of thyroid hormone by deiodinases: local action with general consequences. Cell. Mol. Life Sci. **65**, 570–590

56 Dentice, M. and Salvatore, D. (2011) Deiodinases: the balance of thyroid hormone: local impact of thyroid hormone inactivation. J. Endocrinol. **209**, 273–282

57 Croteau, W., Whittemore, S. L., Schneider, M. J. and St Germain, D. L. (1995) Cloning and expression of a cDNA for a mammalian type III iodothyronine deiodinase. J. Biol. Chem. **270**, 16569–16575

58 Hernandez, A., Fiering, S., Martinez, E., Galton, V. A. and St Germain, D. (2002) The gene locus encoding iodothyronine deiodinase type 3 (*Dio3*) is imprinted in the fetus and expresses antisense transcripts. Endocrinology **143**, 4483–4486

59 Hernandez, A., Martinez, M. E., Croteau, W. and St Germain, D. L. (2004) Complex organization and structure of sense and antisense transcripts expressed from the *DIO3* gene imprinted locus. Genomics **83**, 413–424

60 Dietz, W. H., Masterson, K., Sittig, L. J., Redei, E. E. and Herzing, L. B. (2012) Imprinting and expression of Dio3os mirrors Dio3 in rat. Front. Genet. **3**, 279

61 Derrien, T., Johnson, R., Bussotti, G., Tanzer, A., Djebali, S., Tilgner, H., Guernec, G., Martin, D., Merkel, A., Knowles, D. G. et al. (2012) The GENCODE v7 catalog of human long noncoding RNAs: analysis of their gene structure, evolution, and expression. Genome Res. **22**, 1775–1789

62 Hastings, M. L., Ingle, H. A., Lazar, M. A. and Munroe, S. H. (2000) Post-transcriptional regulation of thyroid hormone receptor expression by *cis*-acting sequences and a naturally occurring antisense RNA. J. Biol. Chem. **275**, 11507–11513

63 Carrieri, C., Cimatti, L., Biagioli, M., Beugnet, A., Zucchelli, S., Fedele, S., Pesce, E., Ferrer, I., Collavin, L., Santoro, C. et al. (2012) Long non-coding antisense RNA controls Uchl1 translation through an embedded SINEB2 repeat. Nature **491**, 454–457

SUPPLEMENTARY ONLINE DATA
Decreased translation of *Dio3* mRNA is associated with drug-induced hepatotoxicity

Kate M. DUDEK*[1], Laura SUTER†, Veerle M. DARRAS‡, Emma L. MARCZYLO§ and Timothy W. GANT§[1]

*Systems Toxicology Group, Medical Research Council Toxicology Unit, University of Leicester, Lancaster Road, Leicester LE1 9HN, U.K., †Institut for Chemistry and Bioanalytics, School of Life Sciences, University of Applied Sciences and Art Northwestern Switzerland (FHNW), Mattenstrasse 22, Basel 4132, Muttenz, Switzerland, ‡Laboratory of Comparative Endocrinology, Department of Biology, Section Animal Physiology and Neurobiology, KULeuven, Naamsestraat 61, PB 2464, Leuven, B-3000, Belgium, and §Centre for Radiation, Chemical and Environmental Hazards, Public Health England, Harwell Campus, Didcot, Oxfordshire OX11 0RQ, U.K.
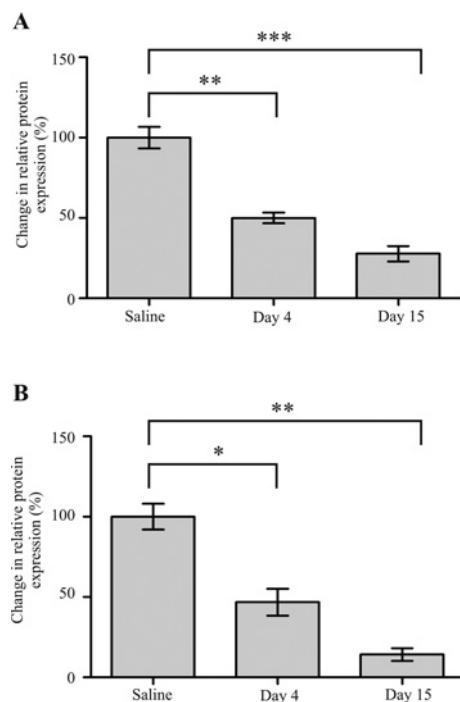
Figure S1   D3 protein is down-regulated in both a time- and dose-dependent manner

Western blot analysis was performed on lysates from the livers of rats treated with various hepatotoxic agents. D3 protein levels were normalized to those of GAPDH. Representative gel images are shown for PredTox compounds FP004BA (**A**) and FP014SC (**B**). Mean relative levels of D3 are indicated beneath each gel image. Results are means $\pm$ S.E.M. ($n = 3$). *$P \leqslant 0.05$, **$P \leqslant 0.01$, ***$P \leqslant 0.001$ (ANOVA with Tukey's/Dunnett's post-hoc test).
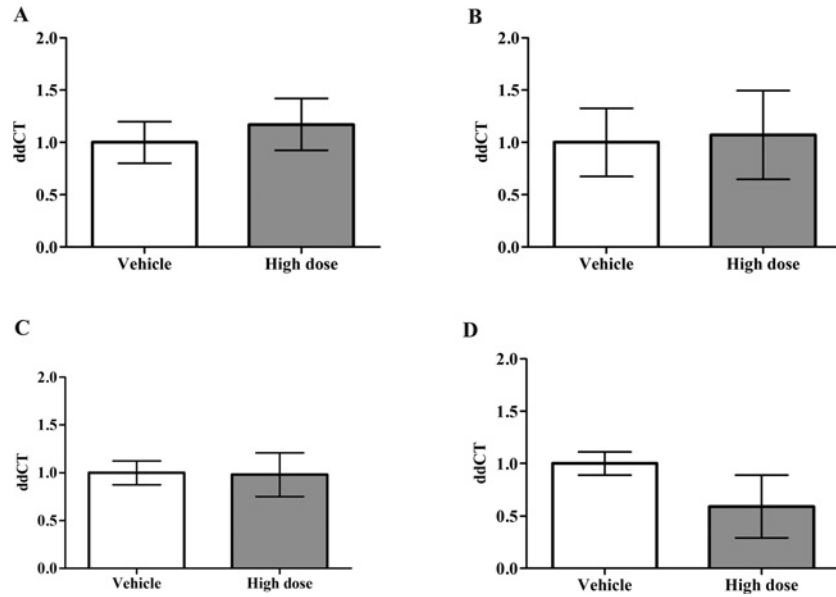
Figure S2   The reduction in D3 protein is not due to changes in mRNA transcription

qRT-PCR analysis was performed on RNA extracted from the livers of rats treated with high doses of PredTox compounds FP004BA (**A**), FP005ME (**B**), FP013NO (**C**) and FP014SC (**D**) for 15 days. Results are means $\pm$ S.E.M. ($n = 3$).
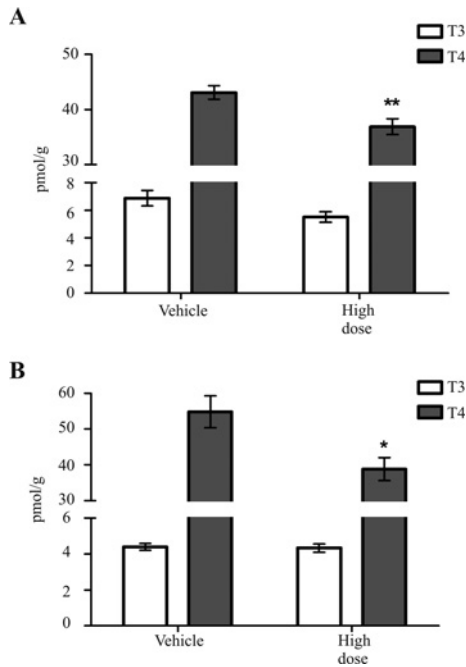
Figure S3   T$_4$ levels within the liver are significantly reduced following drug-induced liver damage

Liver samples were taken for measurement using highly sensitive and specific RIAs following high-dose treatment with PredTox compounds FP004BA (**A**) and FP014SC (**B**). Results represent means $\pm$ S.E.M. ($n \geqslant 3$). *$P \leqslant 0.05$, **$P \leqslant 0.01$ (Student's t test).

A

B

C
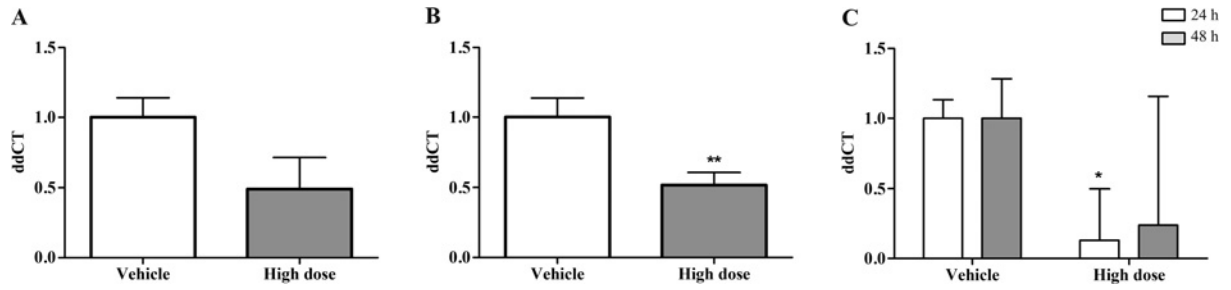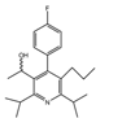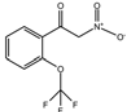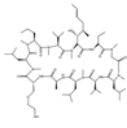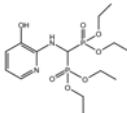
Figure S4   *Dio1* mRNA is transcriptionally down-regulated

qRT-PCR analysis was performed on RNA extracted from the livers of rats treated with high doses of PredTox compounds FP004BA (**A**) and FP007SE (**B**) for 15 days and (**C**) 150 mg/kg thioacetamide. Results are means $\pm$ S.E.M. ($n = 3$). *$P \leqslant 0.05$, **$P \leqslant 0.001$ (Student's *t* test).

Table S1   PredTox compounds and their properties

All available data on the five PredTox compounds selected for further analysis in the present study are provided.

Framework Programme 6 study name	Compound sponsor	Official name	Structure	Proposed high dose (mg/kg)	Proposed low dose (mg/kg)	Target organs	Chemical class	Pharmacological class
FP004BA	Bayer	(+)-(1R)-1-[4-(4-fluorophenyl)-2,6-di-isopropyl-5-propyl-pyridin-3-yl]ethanol		100	20	Liver, kidney	4-Phenylpyridine	Glucagon receptor antagonist
FP005ME	Merck	1-(2-Trifluoromethoxyphenyl)-2-nitroethanone		350	15	Liver	Carbonylnitromethane	Carbonylnitromethanes
FP007SE	Serono	–	–	1000	100	Kidney, liver	–	–
FP013NO	Novartis	–		–	–	–	Cyclosporin derivative	–
FP014SC	Schering	Tetraethyl[(3-hydroxy-2-pyridyl)-amino]-methanediphosphonate		1120	280	Liver	Bisphosphonate	Inhibitor of osteoclast activity

Table S2 Primer sequences

Sequences of primers used to generate *Dio3* and *Actb* probes used in qRT-PCR and PCR experiments.

Gene	Experiment	Direction	Sequence (5′→3′)
Dio3	qRT-PCR	Forward	AGAGTGGCACCATCATGTACCA
		Reverse	CCAAGTGCGCAACTCAGACA
Dio3	PCR and sequencing	Forward	GTGGTCGGAGAAGGTGAA
		Reverse	AGAGGCGCTCAAAATAGG
Actb	qRT-PCR	Forward	CGTGAAAAGATGACCCAGATCA
		Reverse	CACAGCCTGGATGGCTACGT
Actb	PCR	Forward	ATGGTGGGTATGGGTCAGAA
		Reverse	ACATCTGCTGGAAGGTGGAC

Table S3   mRNAs changed in translational activity following treatment with PredTox compound FP014SC

Differentially translated mRNAs were identified following sucrose density fractionation and polysome profiling of liver samples treated with FP014SC. Those mRNAs that showed a statistically significant ($P \leqslant 0.05$) difference in ribosomal occupancy in at least one subpool of fractions when compared with vehicle-treated samples are listed. Significant values are denoted by bold type. *Dio3* is highlighted. Fold changes are colour-coded as indicated in the key.

Fold change key: 3.4 | 1.0 | 0.2

Name	Accession	Monosomes	Polysomes Light	Polysomes Medium	Polysomes Heavy	Translational change	Average mRNA transcript change
Aldob	NM_144903	-1.379	0.023	0.284	1.759	↑	0.17
Rbp4	NM_11255	-0.639	-0.084	0.141	1.418	↑	0.21
Cat	NM_9804	-0.952	-0.572	-0.091	0.918	↑	-0.17
Crp	NM_7768	-1.022	0.012	0.283	0.478	↑	-0.06
Nin	NM_8697	-0.842	0.070	0.033	0.697	↑	-0.01
1700072I22Rik		-0.522	0.084	0.056	0.928	↑	0.14
Fts	BC008130_exon	-0.515	0.080	0.166	0.839	↑	0.14
Spp2	NM_29269	-0.511	-0.186	0.097	0.652	↑	0.01
5930437A14Rik	NM_172542	-0.791	-0.099	0.032	0.395	↑	-0.12
Mug2	NM_8646	-1.032	-0.410	-0.204	0.049	↑	-0.40
Mug1	NM_8645	-0.914	-0.424	0.063	0.057	↑	-0.30
C330046E03		-0.577	0.101	-0.014	0.594	↑	0.03
Samhd1	BC067198_exon	-0.017	0.252	0.342	1.085	↑	0.42
Pgrmc1	NM_16783	-0.657	0.155	-0.111	0.543	↑	-0.02
A230072I16Rik	NM_175004	-0.584	0.275	0.046	0.591	↑	0.08
Kif16a		-0.179	0.138	0.258	0.847	↑	0.27
Ubb	NM_11664	0.514	0.558	0.812	1.473	↑	0.84
Pecr	NM_23523	-0.596	-0.510	-0.001	0.265	↑	-0.21
Mat1a	NM_133653	-0.421	-0.449	-0.029	0.456	↑	-0.11
C530001K22Rik		-0.671	-0.266	-0.153	0.306	↑	-0.20
Syt5	NM_16908	-0.081	0.134	0.397	0.842	↑	0.32
Pou4f1	NM_11143	0.254	0.084	0.396	1.147	↑	0.47
Prop1	NM_8936	-0.356	0.072	0.174	0.581	↑	0.12
Pramel4	NM_178248	0.208	0.115	0.378	1.089	↑	0.45
Hspa8	NM_31165	0.585	1.031	1.437	1.391	↑	1.11
Ass1	NM_7494	-0.301	-0.273	0.230	0.453	↑	0.03
Rad9	NM_11237	-0.296	0.119	0.213	0.593	↑	0.16
3110004H13Rik	NM_26068	-0.117	0.018	0.263	0.718	↑	0.22
4933433G15Rik		-0.195	0.048	0.268	0.644	↑	0.19
2210404O07Rik	XM_125703	0.000	0.306	0.431	0.864	↑	0.40
Kif21b	NM_19962	-0.471	0.107	-0.016	0.461	↑	0.02
4933407H18Rik	XM_132005	-0.211	-0.023	0.092	0.635	↑	0.12
Lu	NM_20486	-0.556	-0.231	-0.106	0.278	↑	-0.15
Bat1a	NM_19693	-0.337	0.105	0.026	0.553	↑	0.09
Imap38	NM_8376	-0.271	0.055	0.201	0.537	↑	0.13
9130221F21	XM_485788	0.817	0.960	0.625	1.778	↑	1.05
BC052055	NM_182636	-0.375	-0.040	-0.082	0.480	↑	0.00
Foxb1	NM_22378	-0.022	0.075	0.203	0.773	↑	0.26
AU016693	NM_178686	-0.299	0.023	0.228	0.461	↑	0.10
Tpcn1	NM_145853	-0.190	-0.021	0.125	0.587	↑	0.13
Sult1a1	NM_133670	-0.644	-0.700	-0.502	0.114	↑	-0.43
Rgs16	NM_11267	-0.350	-0.257	-0.025	0.379	↑	-0.06
Tenc1	BC042190_exon	-0.410	0.162	0.125	0.405	↑	0.07
unknown	AK039504_exon	-0.144	0.364	0.131	0.732	↑	0.27
Clecsf13	NM_16751	-0.275	-0.038	0.118	0.470	↑	0.07
Dfrs4	NM_30686	0.154	0.248	0.520	0.818	↑	0.44
Rac1	NM_9007	-0.356	0.092	0.022	0.412	↑	0.04
4932408F19Rik	NM_207225	-0.419	-0.111	0.004	0.287	↑	-0.06
Map4k6-pending	BC011346_exon	-0.182	0.248	0.161	0.582	↑	0.20
unknown	AF108718_exon	-0.300	-0.019	0.148	0.371	↑	0.05
D3Ertd300e	NM_19995	-0.086	0.091	0.195	0.608	↑	0.20
Camk2b	NM_7595	-0.294	0.119	0.214	0.401	↑	0.11
AI505034	NM_207206	-0.189	0.199	0.122	0.559	↑	0.17
Card10	NM_130859	-0.053	0.083	0.254	0.611	↑	0.22
Peli2	NM_33602	-0.211	0.090	-0.024	0.539	↑	0.10
Atp5g3	NM_175015	0.618	0.859	0.957	1.292	↑	0.93
Centg3	NM_139153	-0.105	0.039	0.221	0.539	↑	0.17
Cd37	NM_7645	-0.290	-0.029	-0.018	0.411	↑	0.02
Kcnc3	NM_8422	-0.157	0.128	0.148	0.526	↑	0.17
Slc29a4	NM_146257	-0.169	0.038	0.180	0.468	↑	0.13
Flih	NM_22009	-0.338	-0.037	0.032	0.313	↑	-0.01
Pak4	NM_27470	-0.255	0.066	0.262	0.347	↑	0.11
unknown	AK085517_exon	-0.419	-0.159	-0.200	0.278	↑	-0.12
1700039I01Rik		-0.354	-0.131	-0.211	0.333	↑	-0.09
Pip5k1c	NM_8844	-0.123	-0.011	0.162	0.463	↑	0.12
0910001L09Rik	NM_132434	-0.236	0.035	0.030	0.407	↑	0.06
C330006A16Rik		-0.177	0.179	0.200	0.457	↑	0.16
D11Ertd18e	NM_26740	-0.035	0.201	0.409	0.534	↑	0.28
A930003A15Rik		-0.223	0.054	0.113	0.393	↑	0.08
Chrna2	NM_144803	-0.447	-0.095	-0.071	0.178	↑	-0.11
Zfp162	NM_11750	0.338	0.354	0.887	0.790	↑	0.59
Ptprn	NM_8985	-0.287	-0.037	-0.056	0.337	↑	-0.01
Dyrk1b	NM_10092	-0.181	0.081	0.097	0.422	↑	0.10
1110059M19Rik	XM_135842	0.381	0.517	0.477	0.996	↑	0.59
Sifl		0.217	0.010	0.188	0.757	↑	0.29
Lgi4	NM_144556	-0.060	0.085	0.203	0.497	↑	0.18
Gm111	NM_207234	-0.148	0.105	0.076	0.455	↑	0.12
Rhbdl6	NM_172572	-0.108	0.120	0.113	0.484	↑	0.15
Apoc1	NM_7469	-0.685	-0.794	-0.718	-0.127	↑	-0.58
Aire	NM_9646	-0.154	0.213	0.164	0.445	↑	0.17
Enah	NM_10135	0.031	0.238	0.204	0.623	↑	0.27
unknown	AK088050_exon	-0.214	0.050	0.131	0.340	↑	0.08
3110007P09Rik	NM_144906	-0.326	-0.018	0.107	0.198	↑	-0.01
Nudt10		0.208	0.326	0.688	0.645	↑	0.47
Sts	NM_9293	-0.175	0.108	0.134	0.374	↑	0.11
Slc2a8	NM_19488	-0.069	0.054	0.112	0.469	↑	0.14
Foxk1	NM_199068	-0.184	0.090	0.078	0.375	↑	0.09
Pcsk2	NM_8792	-0.028	0.092	0.257	0.472	↑	0.20
Kif1c	NM_153103	-0.198	0.017	0.040	0.346	↑	0.05
Nkx6-2	NM_183248	-0.067	0.088	0.173	0.456	↑	0.16
4930471G24Rik		-0.027	0.145	0.233	0.493	↑	0.21
Vdp	NM_19490	-0.304	-0.070	0.009	0.217	↑	-0.04
Brd4	NM_20508	-0.110	0.185	0.083	0.467	↑	0.16
Mrpl24	NM_26591	0.195	0.378	0.448	0.715	↑	0.43
MGC68323	NM_199472	-0.008	0.224	0.736	0.358	↑	0.33
C030046I01Rik	NM_177994	-0.284	-0.055	-0.080	0.259	↑	-0.04
Ptk9l	NM_11876	-0.193	0.020	0.119	0.304	↑	0.06

Name	Accession	Monosomes	Polysomes Light	Polysomes Medium	Polysomes Heavy	Translational change	Average mRNA transcript change
PppIr14a	NM_26731	-0.004	0.230	0.171	0.543	↑	0.23
Pcx	NM_8797	-0.063	0.033	0.138	0.415	↑	0.13
Mrpl49	NM_26246	-0.079	0.198	0.189	0.434	↑	0.19
BC036564	XM_194421	0.127	0.088	0.229	0.588	↑	0.26
Amelx	NM_9666	-0.080	0.170	0.092	0.453	↑	0.16
Apoe	NM_9696	-0.053	0.456	0.390	0.475	↑	0.32
Abcf1	NM_13854	-0.198	0.041	0.155	0.268	↑	0.07
Vtn	NM_11707	-0.736	-0.023	-0.305	-0.141	↑	-0.30
Chdc1	XM_484393	-0.167	0.036	0.006	0.343	↑	0.05
2410022L05Rik	NM_25556	-0.162	-0.059	-0.041	0.329	↑	0.02
Krt1-24	NM_16880	-0.283	-0.158	-0.156	0.212	↑	-0.10
Tub	NM_21885	0.050	0.115	0.259	0.486	↑	0.23
Myo1a		0.150	-0.104	-0.184	-0.307	↓	-0.11
Dusp15	NM_145744	0.830	0.371	0.617	0.262	↑	0.52
Rps5	NM_9095	1.148	0.805	0.637	0.718	↑	0.83
8030442B05Rik		0.020	-0.069	-0.180	-0.435	↓	-0.17
Zan	NM_11741	0.188	-0.106	-0.133	-0.300	↓	-0.09
MoMSVgp1	NC_1502	-0.305	-0.278	-0.444	-0.749	↓	-0.44
Sox1	NM_9233	0.132	0.098	-0.051	-0.320	↓	-0.04
4930448L02Rik		0.021	-0.106	-0.189	-0.457	↓	-0.18
4930557B21Rik		0.027	0.014	-0.140	-0.428	↓	-0.13
1200009I06Rik	NM_28807	-0.061	-0.406	-0.571	-0.514	↓	-0.39
Sphk1	NM_25367	-0.034	0.256	-0.194	-0.392	↓	-0.09
H2-M10.1	NM_13544	0.100	-0.124	-0.340	-0.345	↓	-0.18
Csda	NM_11733	0.603	0.175	0.277	0.044	↑	0.27
Cyp11b2	NM_9991	-0.166	-0.411	-0.390	-0.702	↓	-0.42
Hrg	NM_53176	-0.465	-0.343	-0.679	-0.887	↓	-0.59
Smpd2	NM_9213	0.066	-0.078	-0.151	-0.446	↓	-0.15
2610034P21Rik		-0.017	-0.056	-0.290	-0.481	↓	-0.21
Gfi1	NM_10278	0.191	-0.143	0.018	-0.409	↓	-0.09
Ptgdr	NM_8962	1.087	0.879	0.727	0.590	↑	0.82
4631403P03Rik	NM_153793	-0.071	-0.219	-0.484	-0.531	↓	-0.33
Acex3	NM_30721	-0.049	-0.057	-0.188	-0.555	↓	-0.21
Gnb2-rs1	NM_8143	0.450	0.094	0.088	-0.100	↑	0.13
D15Wsu169e	NM_198420	0.080	-0.116	-0.154	-0.460	↓	-0.16
Mup1	NM_31188	-1.238	-1.816	-2.335	-1.619	↓	-1.75
Hist3h2ba	NM_30082	0.208	-0.167	0.044	-0.417	↓	-0.08
Bcl6b	NM_7528	0.351	0.375	-0.034	-0.071	↑	0.16
AW547186	NM_177592	-0.042	-0.042	-0.082	-0.589	↓	-0.19
Tnnt3	NM_11620	0.049	-0.117	-0.339	-0.439	↓	-0.21
Atf1	NM_7497	-0.139	-0.201	-0.333	-0.660	↓	-0.33
unknown	BC060148_exon	-0.123	-0.230	-0.203	-0.700	↓	-0.31
4930421P22Rik		0.224	0.026	-0.034	-0.338	↓	-0.03
Centa1	NM_172723	0.073	-0.037	-0.349	-0.410	↓	-0.18
1110020A09Rik	NM_27415	-0.191	-0.278	-0.319	-0.768	↓	-0.39
Zcchc3	NM_175126	-0.243	-0.361	-0.382	-0.933	↓	-0.45
B4galt2	NM_17377	-0.132	-0.116	-0.378	-0.644	↓	-0.32
5133400G04Rik	NM_27733	0.028	-0.053	-0.064	-0.579	↓	-0.17
4930405A07Rik		-0.026	-0.055	-0.245	-0.575	↓	-0.23
Fetub	NM_21564	-0.329	-0.419	-0.729	-0.839	↓	-0.58
Tjp3	NM_13769	0.072	-0.225	-0.152	-0.567	↓	-0.22
Ttl	NM_27192	0.096	-0.172	-0.164	-0.537	↓	-0.19
Mup4	NM_8648	-1.181	-1.653	-2.342	-1.597	↓	-1.69
2010012O05Rik	NM_25563	-0.001	-0.119	-0.106	-0.655	↓	-0.22
2300003C06Rik	NM_28001	0.221	0.184	-0.053	-0.351	↓	0.00
Fgf23	NM_22657	0.206	0.111	-0.042	-0.396	↓	-0.03
Foxo6	NM_194060	-0.030	-0.120	-0.120	-0.690	↓	-0.24
2510015F01Rik	XM_354801	0.120	0.070	-0.119	-0.480	↓	-0.10
Cyp2c50	NM_134144	0.242	0.167	-0.126	-0.328	↓	-0.01
Tubb4	NM_9451	-0.451	-0.513	-0.522	-1.124	↓	-0.65
Notch4	NM_10929	0.088	0.016	-0.148	-0.541	↓	-0.15
5830428M24Rik	XM_488638	0.050	-0.160	-0.247	-0.612	↓	-0.24
Rpl21	NM_19647	1.219	1.236	0.723	0.699	↑	0.97
4930441N18Rik		0.036	-0.112	-0.373	-0.573	↓	-0.26
Nr2f6	NM_10150	-0.137	-0.334	-0.410	-0.809	↓	-0.42
r171.1	NC_2512	0.028	-0.122	-0.260	-0.630	↓	-0.25
Banfl	NM_11793	-0.137	-0.124	-0.346	-0.769	↓	-0.34
D5Ertd708e	NM_24216	0.282	-0.028	-0.071	-0.413	↓	-0.06
3110052M02Rik	XM_484601	-0.370	-0.173	-0.254	-1.071	↓	-0.47
Myes	NM_10850	-0.018	-0.102	-0.199	-0.723	↓	-0.26
1110007A13Rik	NM_145955	0.024	-0.109	-0.169	-0.700	↓	-0.24
Pold1	NM_11131	0.259	-0.191	-0.199	-0.483	↓	-0.15
Cyp2j13	NM_145548	-0.444	-1.054	-1.297	-1.118	↓	-0.98
Park2	NM_16694	-0.216	-0.363	-0.565	-0.910	↓	-0.51
Zcchc3	NM_175126	-0.069	-0.219	-0.263	-0.821	↓	-0.34
Sumo1	NM_9460	-0.174	-0.208	-0.022	-1.009	↓	-0.35
Zdhhc21	NM_26647	-0.017	-0.303	-0.487	-0.736	↓	-0.39
A930033C23Rik		0.108	0.011	-0.084	-0.649	↓	-0.15
2410187C16Rik	XM_128102	0.914	0.131	0.195	0.075	↑	0.33
2610301G19Rik	BC021475_exon	-0.229	-0.253	-0.357	-1.016	↓	-0.46
3110052M02Rik	XM_484601	-0.006	-0.372	-0.151	-0.904	↓	-0.36
Eif3s4	NM_16876	0.120	-0.024	-0.189	-0.675	↓	-0.19
Gja9	NM_10290	0.287	-0.159	-0.128	-0.583	↓	-0.15
3110009E18Rik	NM_28439	-0.073	-0.379	-0.237	-0.987	↓	-0.42
unknown	BC065789_exon	0.006	-0.135	-0.205	-0.824	↓	-0.29
4930563H03Rik		-0.352	-0.680	-0.915	-1.175	↓	-0.78
Plvap	NM_32398	-0.072	-1.015	-0.595	-1.120	↓	-0.70
Uchl1	NM_11670	-0.010	-0.052	-0.293	-0.874	↓	-0.31
4933434G05Rik	XM_126681	-0.066	-0.212	-0.131	-1.078	↓	-0.37
Orc5l	NM_11959	0.162	-0.296	-0.119	-0.895	↓	-0.29
4930438O05Rik	NM_27507	0.103	-0.221	-0.130	-0.939	↓	-0.30
2410080H04Rik	NM_172522	0.066	-0.594	-0.341	-1.055	↓	-0.48
Arl2bp	NM_24191	0.155	-0.261	0.009	-0.978	↓	-0.27
Tcirg1	NM_16921	-0.210	-0.381	-0.472	-1.246	↓	-0.58
Pin1	NM_23371	0.223	-0.181	-0.109	-0.940	↓	-0.25
Narfl	NM_26238	0.260	-0.565	-0.167	-1.026	↓	-0.37
B230208J24Rik	NM_145356	-0.136	-0.443	-0.407	-1.309	↓	-0.57
Dio3	NM_172119	-0.396	-0.602	-0.775	-1.508	↓	-0.82
1700095D23Rik		0.128	-0.315	-0.476	-1.053	↓	-0.43
Fstl1	NM_8047	-0.078	-0.517	-0.810	-1.268	↓	-0.67
Serpina3c	NM_8458	0.215	-0.169	-0.809	-0.927	↓	-0.42
Arrdc2	XM_134227	-0.012	-0.292	-0.197	-1.478	↓	-0.49
Pacs1	NM_153129	-0.042	-0.151	-0.334	-1.435	↓	-0.49
Cmkor1	NM_7722	0.241	-0.233	0.131	-1.447	↓	-0.33

Table S4 Canonical pathways that were significantly perturbed (two or more genes) following treatment with PredTox compound FP014SC

All mRNAs that showed a change in ribosomal occupancy across the gradient following polysome profiling were uploaded for pathway analysis to Ingenuity® IPA software. Those pathways under the control of RXR are in bold (FXR, farnesoid X receptor; IL-1, interleukin 1; LPS, lipopolysaccharide; LXR, liver X receptor; PPARα, peroxisome-proliferator-activated receptor α; PXR, pregnane X receptor).

Ingenuity® canonical pathway	$-\log(P \text{ value})$	Number of altered genes
Fatty acid metabolism	8.71	15
LPS/IL-1 mediated inhibition of RXR function	2.67	10
Production of nitric oxide and reactive oxygen species in macrophages	3.10	10
Clathrin-mediated endocytosis signalling	2.99	10
G-protein-coupled receptor signalling	0.319	9
mTOR signalling	2.47	9
Axonal guidance signalling	0.689	9
Glucocorticoid receptor signalling	1.51	9
Tryptophan metabolism	2.81	8
Protein kinase A signalling	0.834	8
PPARα/RXRα activation	2.11	8
Metabolism of xenobiotics by cytochrome P450	3.18	8
LXR/RXR activation	3.15	8
RAR activation	2.11	8
eIF2 signalling	1.94	8
Regulation of eIF4 and p70^{S6K} signalling	2.57	8
Protein ubiquitination pathway	1.16	8
PI3K signalling in B-lymphocytes	2.14	7
Role of macrophages, fibroblasts and endothelial cells in rheumatoid arthritis	0.613	7
Molecular mechanisms of cancer	0.475	7
Calcium signalling	1.58	7
Xenobiotic metabolism signalling	0.718	7
Dopamine–DARPP32 feedback in cAMP signalling	1.71	7
ERK/MAPK signalling	1.47	7
Acute-phase response signalling	1.67	7
Valine, leucine and isoleucine degradation	3.11	6
CREB signalling in neurons	1.17	6
B-cell receptor signalling	1.48	6
Breast cancer regulation by Stathmin1	0.981	6
Wnt β-catenin signalling	1.19	6
Bile acid biosynthesis	3.58	6
Arachidonic acid metabolism	1.75	6
RhoGDI signalling	0.773	5
Ephrin receptor signalling	0.794	5
Huntington's disease signalling	0.530	5
Purine metabolism	0.330	5
Linoleic acid metabolism	2.07	5
Glycolysis/gluconeogenesis	1.81	5
Fatty acid elongation in mitochondria	4.93	5
Phospholipase C signalling	0.468	5
Atherosclerosis signalling	1.33	5
IL-12 signalling and production in macrophages	1.15	5
Actin cytoskeleton signalling	0.554	5
Sertoli cell–Sertoli cell junction signalling	0.745	5
Semaphorin signalling in neurons	1.97	4
NRF2-mediated oxidative stress response	0.457	4
P2Y purigenic receptor signalling pathway	0.848	4
Tyrosine metabolism	1.46	4
Pyruvate metabolism	1.62	4
Human embryonic stem cell pluripotency	0.753	4
GNRH signalling	0.821	4
Role of NFAT in cardiac hypertrophy	0.439	4
Synaptic long-term potentiation	1.02	4
Colorectal cancer metastasis signalling	0.250	4
Glioblastoma multiforme signalling	0.623	4
PI3K/Akt signalling	0.867	4
PTEN signalling	0.979	4
Hereditary breast cancer signalling	0.886	4
Tight junction signalling	0.585	4
IL-8 signalling	0.491	4
Glycerolipid metabolism	1.05	4
FXR/RXR activation	1.25	4
Inositol phosphate metabolism	0.616	4
AMPK signalling	0.737	4
Mitochondrial dysfunction	0.737	4
Type 2 diabetes mellitus signalling	0.906	4

Table S4   Continued

Ingenuity® canonical pathway	— log (*P* value)	Number of altered genes
Ceramide signalling	1.39	4
Aldosterone signalling in epithelial cells	0.579	4
Amyotrophic lateral sclerosis signalling	1.08	4
Signalling by Rho family GTPases	0.266	4
Sphingosine 1-phosphate signalling	0.926	4
Germ cell–Sertoli cell junction signalling	0.573	4
p38 MAPK signalling	0.590	3
Circadian rhythm signalling	1.84	3
FGF signalling	0.787	3
Pentose and glucuronate interconversions	1.55	3
GM-CSF signalling	1.08	3
Neuropathic pain signalling in dorsal horn neurons	0.605	3
iCOS–iCOSL signalling in T-helper cells	0.590	3
PKCθ signalling in T-lymphocytes	0.526	3
Prostate cancer signalling	0.820	3
Cyclins and cell-cycle regulation	0.843	3
Aryl hydrocarbon receptor signalling	0.401	3
Small-cell lung cancer signalling	0.944	3
Thyroid cancer signalling	1.44	3
Non-small-cell lung cancer signalling	1.03	3
Retinol metabolism	1.44	3
TR/RXR activation	0.777	3
Galactose metabolism	1.47	3
Alanine and aspartate metabolism	1.55	3
Dendritic cell maturation	0.304	3
OX40 signalling pathway	0.766	3
Cdc42 signalling	0.293	3
Type 1 diabetes mellitus signalling	0.567	3
Insulin receptor signalling	0.437	3
Natural killer cell signalling	0.605	3
Oxidative phosphorylation	0.368	3
Role of Oct4 in mammalian embryonic stem cell pluripotency	1.42	3
Cardiac β-adrenergic signalling	0.426	3
fMLP signalling in neutrophils	0.575	3
CCR3 signalling in eosinophils	0.533	3
CXCR4 signalling	0.330	3
Paxillin signalling	0.629	3
LPS-stimulated MAPK signalling	0.917	3
Regulation of actin-based motility by Rho	0.787	3
Rac signalling	0.605	3
p70^{S6K} signalling	0.476	3
NGF signalling	0.605	3
Androgen and oestrogen metabolism	0.832	3
Sulfur metabolism	2.38	3
Fructose and mannose metabolism	1.30	3
Renal cell carcinoma signalling	0.958	3
Hypoxia signalling in the cardiovascular system	1.00	3
RhoA signalling	0.258	2
Neurotrophin/Trk signalling	0.498	2
ATM signalling	0.671	2
Arginine and proline metabolism	0.466	2
Ubiquinone biosynthesis	0.490	2
Basal cell carcinoma signalling	0.490	2
Factors promoting cardiogenesis in vertebrates	0.372	2
Role of Nanog in mammalian embryonic stem cell pluripotency	0.266	2
Glioma signalling	0.329	2
Melatonin signalling	0.474	2
Urea cycle and metabolism of amino groups	1.01	2
Oestrogen-dependent breast cancer signalling	0.581	2
p53 signalling	0.339	2
Bladder cancer signalling	0.361	2
Androgen signalling	0.254	2
Cell cycle: G$_1$/S checkpoint regulation	0.624	2
Chronic myeloid leukaemia signalling	0.334	2
Cell cycle regulation by BTG family proteins	0.942	2
HGF signalling	0.309	2
Pancreatic adenocarcinoma signalling	0.278	2
PXR/RXR activation	0.498	2
IL-1 signalling	0.344	2
Glutamate receptor signalling	0.613	2

Table S4   Continued

Ingenuity® canonical pathway	— log (*P* value)	Number of altered genes
Butanoate metabolism	0.581	2
Telomerase signalling	0.305	2
Cross-talk between dendritic cells and natural killer cells	0.355	2
Cytotoxic T-lymphocyte-mediated apoptosis of target cells	0.409	2
Allograft rejection signalling	0.397	2
Caveolae-mediated endocytosis signalling	0.458	2
Virus entry via endocytic pathways	0.355	2
Neuroprotective role of THOP1 in Alzheimer's disease	0.848	2
FcεRI signalling	0.291	2
PDGF signalling	0.482	2
CD40 signalling	0.552	2
TNFR1 signalling	0.724	2
Angiopoietin signalling	0.533	2
Parkinson's disease signalling	1.45	2
Apoptosis signalling	0.361	2
Retinoic acid-mediated apoptosis signalling	0.552	2
Citrate cycle	1.08	2
Activation of IRF by cytosolic pattern recognition receptors	0.552	2
Dopamine receptor signalling	0.444	2
CDK5 signalling	0.372	2
Regulation of IL-2 expression in activated and anergic T-lymphocytes	0.423	2
CD28 signalling in T-helper cells	0.240	2
Agrin interactions at neuromuscular junctions	0.507	2
FAK signalling	0.372	2
PAK signalling	0.361	2
Renin–angiotensin signalling	0.266	2
Role of BRCA1 in DNA damage response	0.624	2
Sphingolipid metabolism	0.397	2
Keratan sulfate biosynthesis	0.635	2
Inositol metabolism	2.41	2
G-protein signalling mediated by Tubby	0.963	2
14-3-3-mediated signalling	0.226	2
Starch and sucrose metabolism	0.507	2